www.s2is.org
International Journal on Smart Sensing and Intelligent Systems
ISSN 1178-5608

# A ST X-NUCLEO-BASED TELEMETRY UNIT FOR DETECTION AND WiFi TRANSMISSION OF COMPETITION CAR SENSORS DATA: FIRMWARE DEVELOPMENT, SENSORS TESTING AND REAL-TIME DATA ANALYSIS

P. Visconti[1], B. Sbarro[2], P. Primiceri[3]

Department of Innovation Engineering, University of Salento, 73100, Lecce, Italy
Emails: paolo.visconti@unisalento.it [1], bernardo.sbarro@studenti.unisalento.it [2]
patrizio.primiceri@unisalento.it [3].

***Submitted: Aug. 21, 2017 Accepted: Nov. 1, 2017 Published: Dec. 1, 2017***

***Abstract – Telemetry is a technology that allows remote measurement and transmission of moving car information, allowing to collect a huge amount of data that are interpreted to ensure that car is performing at its optimum. In this research work, by using electronic modules and sensors available at very low costs, a reliable and accurate telemetry system was realized in order to monitor physical and mechanical parameters of a racing vehicle during its motion. Implemented data acquisition and wireless communication unit allows to collect, on board of vehicle, the temperature of engine compartment and cooling liquid, suspensions' extensions, vehicle speed and also its orientation and acceleration and to send wirelessly all these data to a base station, where are monitored by technical staff, so ensuring quick intervention in case of malfunctioning. STM32 Nucleo development board, heart of realized telemetry system, properly programmed with the developed firmware, acquires data from used sensors and, through a WiFi radio module, sends them to the base station; the data are also stored on a SD memory card to avoid data losses. Sparkfun CAN module is employed for this aim and to interface the engine control unit with ST Nucleo board. Experimental tests were carried out for verifying correct operation of realized system; by analyzing trends over time of monitored vehicle parameters as function of the vehicle movements, driving conditions and race track, the technicians ensure safety of pilot life and also an optimization of the vehicle performances.***

**Index terms: Telemetry, sensors, electronic modules, firmware, wireless monitoring, prototype testing.**

# I. INTRODUCTION

Nowadays electronics field, even more open source, offers increasingly possibility to users and designers to create smart systems featured by high performance, advanced functionalities but low costs. These opportunities are becoming highly appreciated in the automotive field and in particular in the highly competitive environment of car races where the embedded electronic systems are playing an increasingly important role with the possibility to monitor and control, in real time and continuously, all phisical and mechanical parameters characterizing vehicle movement [1-3], so allowing to safeguard pilot life and optimize the vehicle performances. *Formula SAE* was established by the *Society of Automotive Engineers* (SAE) in 1981 and consists of a periodically organized competition between academic teams, including the *Salento University* one, which compete in the design, construction and testing of prototype single-seater cars [4].

A telemetry system, applied to a common or racing car, allows to monitor driving conditions and the physical and mechanical parameters values, to compare real-time these data and thus to intervene if some anomalies are present. In this research work, as shown in Figure 1, the realized system is able to collect data related to the mechanical system and vehicle dynamics during its motion, and to send them, wirelessly, to a base station to be monitored, in real time, by the engineers. Different sensors mounted on vehicle are employed to detect the parameters of interest and exchange wirelessly these data through the telemetry electronic boards.

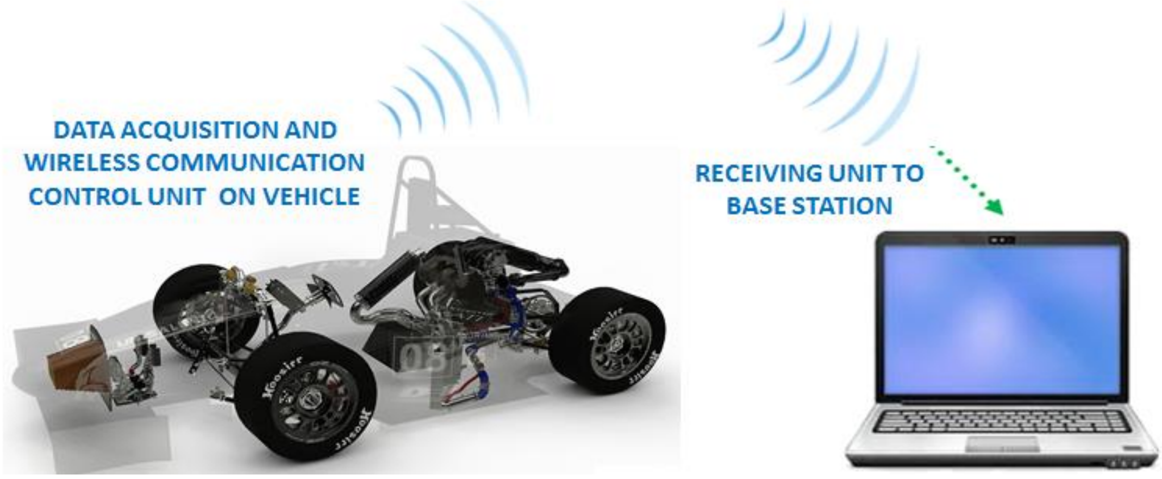

Figure 1. Image of the FSAE SRT16 single-seater prototype realized by *Salento Racing Team* with the mechanical system in evidence; the telemetry system, installed on the vehicle, sends the sensors data, related to the vehicle parameters, to the base station to be monitored.

The STM-32 X-Nucleo F411RE development board is the central unit of the realized electronic system; properly programmed with the developed firmware, it acquires the data provided by the sensors installed on vehicle and, by using a WiFi radio module, sends them to a base station [5-9]. Here, another STM-32 Nucleo board, connected with PC via USB cable, receives the data by means of a further WiFi radio module and displays them on the PC terminal [10-12]. The detected sensors data are also stored, on board of the vehicle, on a SD memory card hosted by the Sparkfun CAN BUS module, thus allowing to have a robust and reliable telemetry system which keeps data even if the wireless transmission fails. The carried out experimental tests showed that realized telemetry system is able to acquire properly the sensors data related to vehicle paramaters and to send them to the base station. The received data are in accordance between themselves; the engine temperature values, vehicle speed, suspensions' extension are function of vehicle movements, driving and track conditions.

## II. TELEMETRY SYSTEMS AVAILABLE ON THE MARKET FOR AUTOMOTIVE FIELD

Nowadays, vehicle tracking and telemetry systems are required by many companies operating in the car manufacturing with the aim to improve vehicle performences and provide high security and comfort levels for the pilot and passengers. Different telemetry systems exist in commerce, each of them with specific characteristics and costs. The advanced technologies have facilitated the realization of sophisticated but also reliable and robust telemetry devices. Following, some of recent telemetry systems, developed by leader companies in the field, are described with their main technical features. The *CAEMAX* company developed a complex telemetry system, named *D*$^x$, based on universal transmission modules that allow to carry out measurements using a multi-channel system and different sensor assignments (Figure 2) [13].

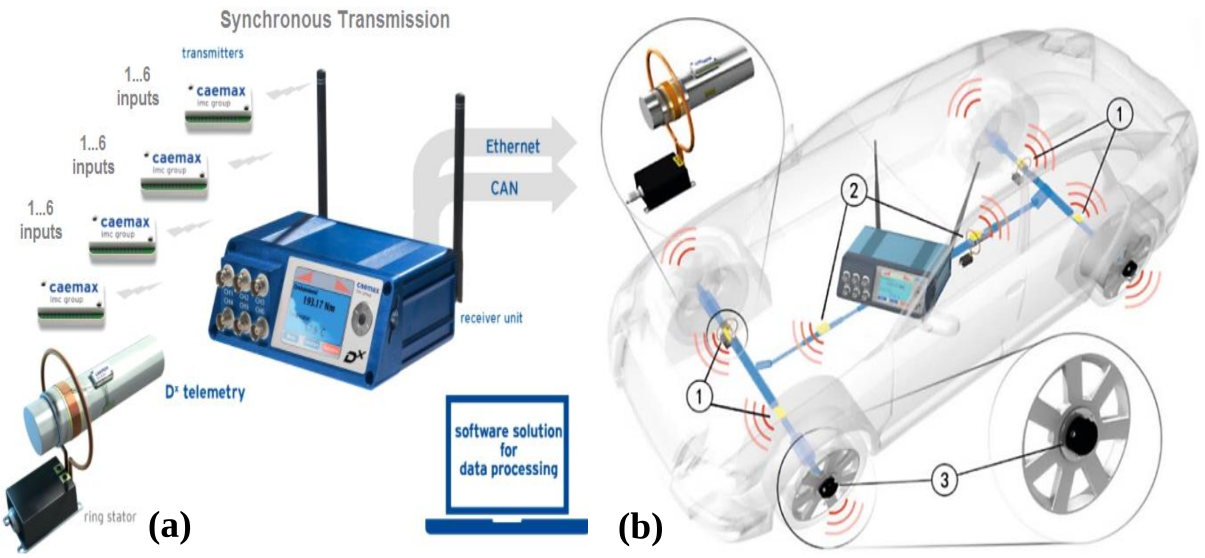

Figure 2. CAEMAX D$^x$ telemetry system guarantees simultaneous data acquisition from multiple sensors mounted on the vehicle (a) and image of CAEMAX D$^x$ rotating components positioned in different sectors of the vehicle for monitoring acceleration, force and torque (b).

The telemetry apparatus, through a synchronous operation of different transmitter modules and a central receiver unit (Figure 2a), guarantees simultaneous data acquisition from multiple sensors, located in different sections of vehicle, as shown in Figure 2b. CAEMAX $D^x$ system digitizes the analog sensor signals for detecting temperature, strain gauge, acceleration, force and torque in the transmitter unit; furthermore, a redundant error detection ensures that only correct data are transmitted. The same transmitter can be used for different types of sensors (strain gauges, thermocouples, accelerometers) and for multiple acquisition channels.

Advanced telemetry systems for automotive applications are developed by KTM company; these systems consist of 1-channel telemetry for rotating shafts, point-to-point telemetry, rotating telemetry for wheels and rotors and thermo telemetry, each of them featured by proper devices for the specific application [14]. For example, a torque sensor, produced by CAEMAX, is used on steering wheel, as shown in Figure 3, for monitoring torque, steering angle and rotational velocity. It also can acquire acceleration in the center of the steering column (x, y and z directions) as well as the rotational acceleration. The measurement data are digitized with a resolution of 16 bits, reaching a precision of torque measurement of 0.1% FS.

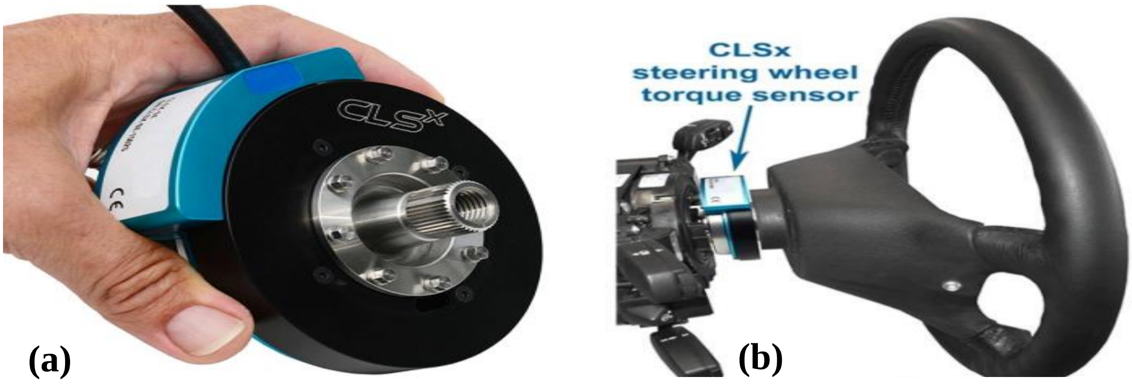

Figure 3. CAEMAX $D^x$ torque sensor (a) placed between steering column and multi-functional steering wheel (b) used to evaluate the steering torque and steering angle while driving.

Rotate telemetry systems are suitable for the toughest conditions such as brake testing on wheel rims of vehicles and trucks. The waterproof systems enable the collection, processing and transmission of 2, 4, 8, 16 and 32 parallel strain and/or thermo signals from the rotor. The processed and digitized signal with 12/16 bit resolution is transferred, by means of a special HF radio link, to the receiver unit over distances of up to 10m and digital data transmission rates up to 2.500 kbit/s. As example, a latest generation device is the *CTP4/8-Rotate*, produced by *KTM*, for high dynamic measurements on wheels or rotors (Figure 4) [15]. The CTP8-Rotate is a programmable 4/8-channel telemetry system specifically designed to be mounted on rotating wheels or rotors of helicopters. To the devices can be connected different sensors: strain gauges, type-K thermocouples, integrated circuit piezoelectric (ICP) sensors or capacitive sensors. The acquired signals are digitized and transmitted via WiFi transmission to a stationary receiver located inside the vehicle or helicopter cabin. Four different carrier frequencies are provided, thus allowing up to four systems (e.g for four wheels) to operate in parallel. The complete transmitter assembly is water-proofed to IP65 specifications.

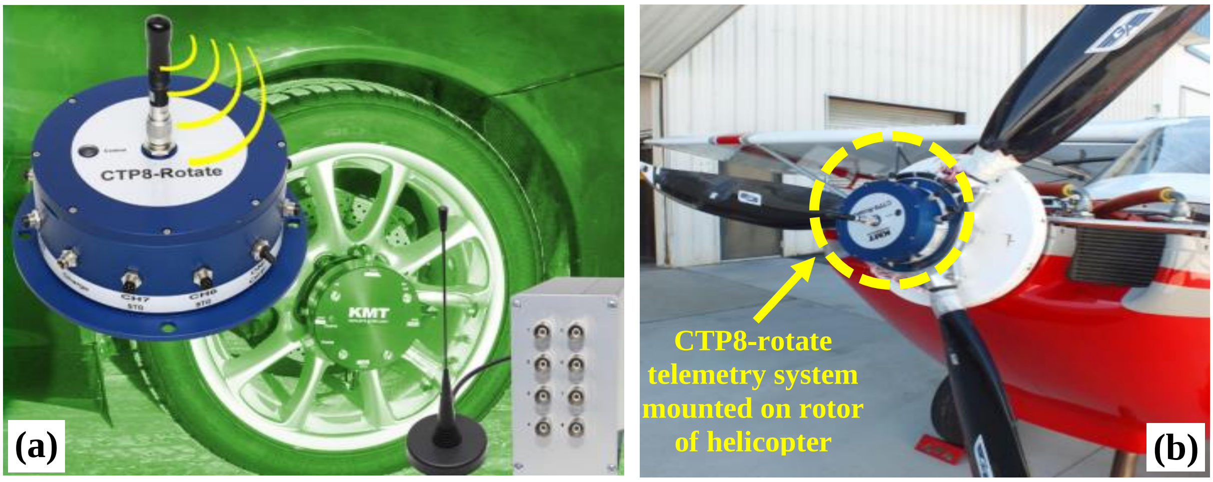

Figure 4. CTP4/8-Rotate applied on a vehicle wheel (a) or on the rotor of a helicopter (b).

The maximum distance between transmitter and receiving antennas is about 10-20m, as declared by KTM company. Furthermore, the CTP4/8-Rotate telemetry enables an extreme high-speed signal transfer, up to 5Mbit/s; so, all channels can be transferred with an analogue bandwidth, up to 12kHz, very important in measurements of torque and vibrations [15].

Magneti-Marelli is another company leader in the production of hi-tech telemetry systems for engine control and data acquisition (*Engine Control Units*, *ECUs*) as well as electro-hydraulic systems for gear box automation and control [16]. For telemetry related to racing vehicle (Figure 5), sensors measure several parameters among which the number of laps or brakes temperature; the measurements are then sent to a data logger which stores them on an internal memory. Data are then transmitted via radio to the base station, for remote and real-time vehicle monitoring during the competition. The telemetry at this level is really sophisticated: a racing vehicle is monitored in all its parts, moment by moment; on a *Formula 1* car, more than a thousand parameters are acquired, with sampling times ranging from one reading/sec to more than 100.000 readings/sec. The acquired data are related to many different parameters: temperature of brakes, water-oil-fuel levels, engine operation (RPM value, fuel injection and pressure, ignition times), transmission and mechanical parts, pressure of hydraulic systems, as well as data coming from the chassis such as suspensions, pressure on aerodynamic parts, all data concerning transmission, tyres, stability, balancing under braking, etc.

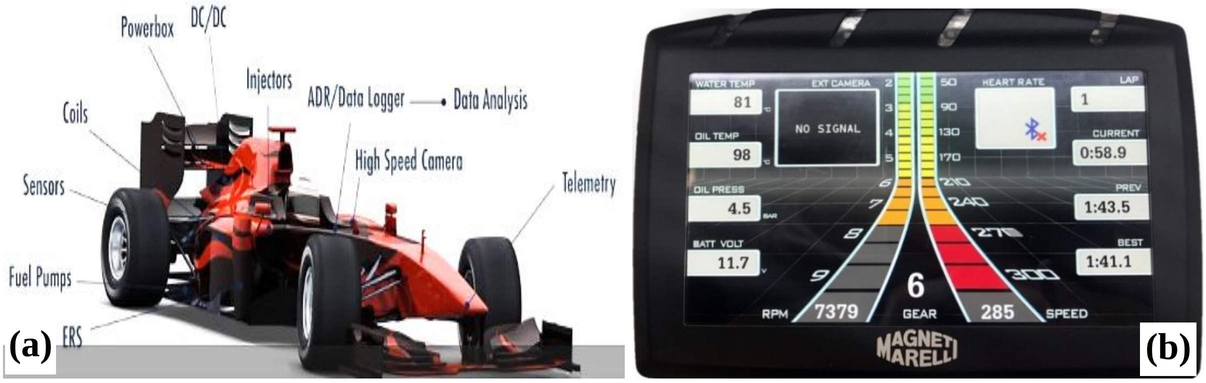

Figure 5. Racing vehicle monitored via radio in all its parts; data received from base station are analyzed in real time by engineers (a) and a dashboard, produced by Magneti Marelli, for use either as a stand-alone display unit or as integral part of the data monitoring system (b).

All these information are downloaded at the end of the trial or race, or received in real time via radio and analysed by team experts. Figure 5 reports the dashboard, realized by Magneti Marelli, for use either as a stand-alone display unit or as integral part of the data acquisition and monitoring system. The dashboard can communicate by a Controller Area Network (CAN) with a range of additional data loggers receiving and displaying data from the logger. On-board, the Wi-Fi and BLE connection modules (with internal antennas) allow a large variety of connections, starting like PC/tablet link for setup and data analysis [16].

Another leader company, *Accumetrics*, presents sophisticated telemetry systems where torque, temperature, vibration, and strain values can be transmitted off rotating shafts using reliable digital wireless techniques. Single and multi-channel systems, both induction and battery powered, allow to solve challenging automotive test requirements; as example, to measure average and high bandwidth torque phenomena, proposed device is the *AT-5000 EasyApp* (Figure 6). It utilizes a small battery powered transmitter mounted using an aramid fiber strap to directly measure, digitize and transmit torque data from rotating half-shafts, drive-shafts and rotors. The system is also used for temperature, voltage, and acceleration sensing [17].

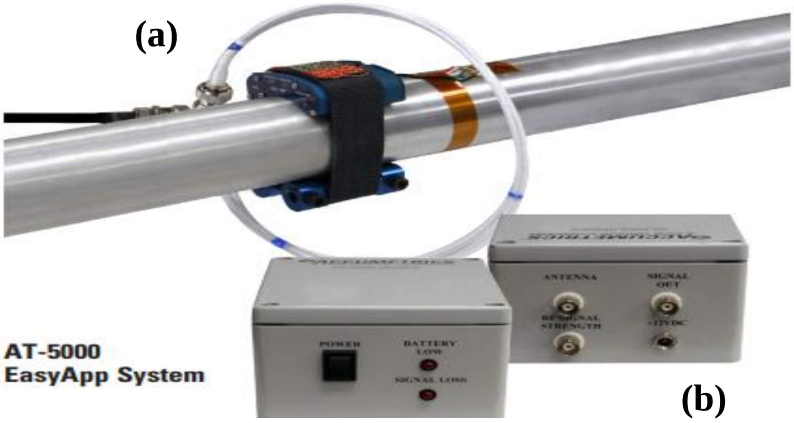

Figure 6. AT-5000 transmitter (a) and receiver units (b) installed on a rotating shaft.

Telemetry system, developed by *Accumetrics*, uses a long life lithium battery to excite a strain gage and to power the AT-5000 telemetry electronics on the rotating shaft. The small signal resulting from torque applied to the shaft is amplified, filtered and digitized (typically at 11718 samples per second). The digital data are reliably RF transmitted off the rotating shaft to a nearby pickup coil, which is connected to a receiver. This last converts the digital data to an analog output voltage, with amplitude adjustable from ± 1 up to ± 10 Volts and frequency from 0 up to 1 kHz (or optionally higher), that can be provided directly to a data acquisition system, to a FFT analyzer for data/signal processing or to an oscilloscope for data viewing.

Many other companies, leader in the market of telemetry systems, produce increasingly advanced devices thanks to the research in this sector and to achieved technological advances in the last years. In the next paragraphs, the telemetry system realized in this research work is illustrated; it was realized, contrarily to the telemetry systems reported above, using devices available on the market at very low costs but able to implement a telemetry system robust and reliable, for monitoring of the main parameters of the competition vehicle during its motion.

## III. PRINCIPAL BLOCKS OF REALIZED SYSTEM AND OPERATING MODE

The data acquisition and transmission section is the central unit of the realized telemetry system; it allows to analyze the performance of vehicle and to constantly monitor its status during competitions. For collecting all data provided by sensors and to transmit them wirelessly to the remote base station, different modules and devices connected to the mechanical system of the vehicle and electronically between them are used. The block diagram of Figure 7 reports the connections between the different sensors and data acquisition and transmission section; the connections are made directly or through the engine control unit.

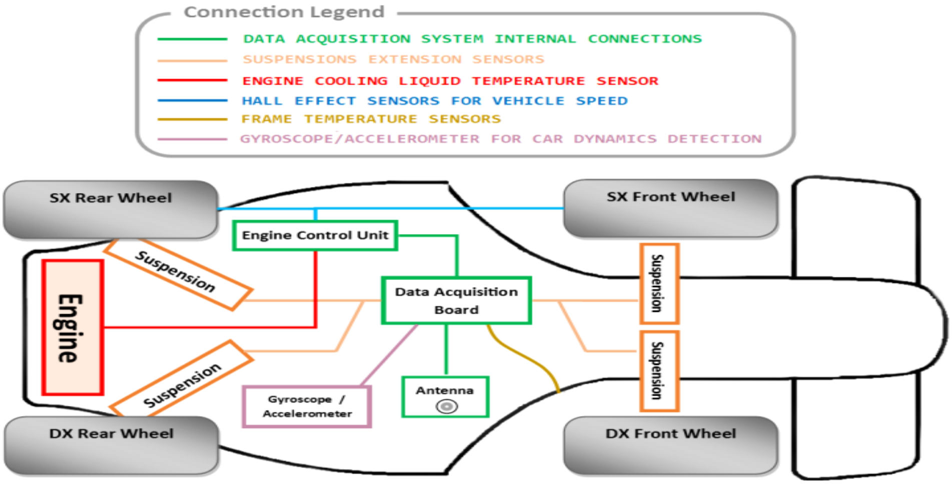
Connection Legend
DATA ACQUISITION SYSTEM INTERNAL CONNECTIONS
SUSPENSIONS EXTENSION SENSORS
ENGINE COOLING LIQUID TEMPERATURE SENSOR
HALL EFFECT SENSORS FOR VEHICLE SPEED
FRAME TEMPERATURE SENSORS
GYROSCOPE/ACCELEROMETER FOR CAR DYNAMICS DETECTION
SX Rear Wheel
SX Front Wheel
Engine Control Unit
Suspension
Engine
Data Acquisition Board
Suspension
Suspension
Suspension
Gyroscope / Accelerometer
Antenna
DX Rear Wheel
DX Front Wheel

Figure 7. Block diagram of the designed electronic system for sensors data acquisition and wireless transmission, through WiFi connection, implemented on the FSAE vehicle.

The data detected by sensors are stored and sent wirelessly, through WiFi transmission module assembled on STM Nucleo board, as shown in Figure 8; the whole electronic system is composed of different modules described following, electronically interconnected and with specific features. One of these modules is the conditioning board that represents the interface between sensors installed on vehicle and the other modules; it is provided of two black connectors for sensors connection, two sockets for assembling of the STM Nucleo-F411RE board and Sparkfun CAN-BUS module and of electronic components for adapting of the signals levels provided from sensors, as required by the Nucleo board input pins.

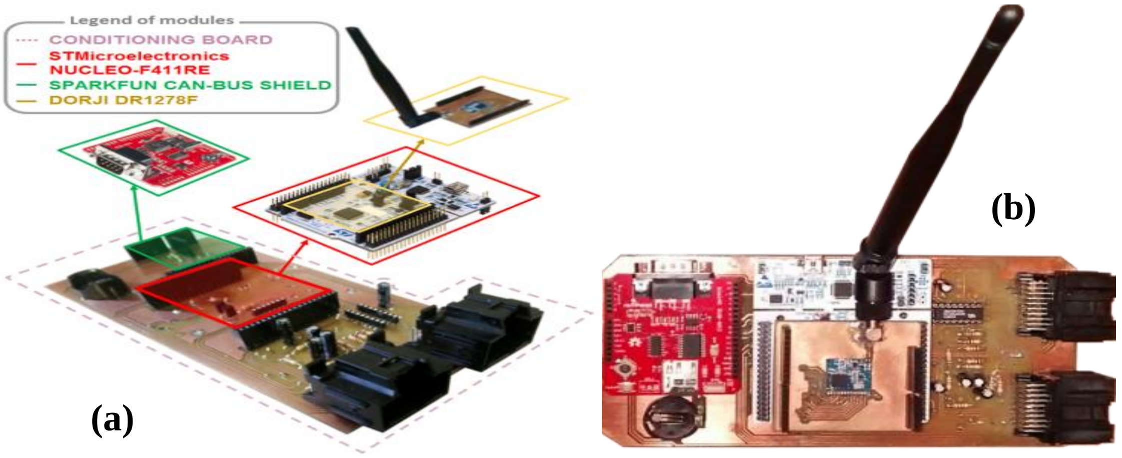

Figure 8. Realized telemetry system for data acquisition/transmission via WiFi connection; different modules disassembled and their interconnections on the signals conditioning board (a) and the complete system with all modules properly assembled and connected (b).

The ST F411RE Nucleo board, a programmable board for rapid prototyping based on STM32 microcontroller, is the central unit; it receives the sensors data, directly or through the Sparkfun CAN module. The directly connected sensors are the following:

- ✓ four IXTHUS PZ-12-A-75P linear potentiometers connected to vehicle suspensions for detecting their extension; in this way, it is possible to monitor the suspension behavior and vehicle stability, thus avoiding functional asymmetries during the car motion;
- ✓ four LM35 temperature sensors located inside the engine compartment, in particular, two close to the engine discharge and the other two on the right and on left side of the engine;
- ✓ one MPU6050 gyroscope/accelerometer, located at center of the mechanical structure of vehicle, for detecting acceleration and inclination angles (i.e. pitch, roll and yawing), during vehicle motion. Thus, it is possible to control the vehicle weight distribution on the axes and so to adjust the suspensions system for improving the vehicle performances.

The sensors connected to the engine control unit and, through it, to the data acquisition board (namely the ST X-Nucleo board), are the following:

- ✓ one NTC thermistor for acquiring the cooling liquid temperature, thus monitoring the operating temperature of the mechanic sections;
- ✓ two Cherry GS1001 Hall effect sensors, located on the front and rear wheels on the left side of the vehicle, for determining the vehicle speed and any slippage between wheels. These sensors are positioned perpendicularly to a particular gear wheel, named phonic wheel, united with vehicle wheel itself. In this way, Hall sensors detect the passage of each tooth of the wheel and, consequently, they keep track of the wheel angular speed.

The Sparkfun CAN-BUS module is used for interfacing ST Nucleo board and engine control unit and, in addition, to store detected sensors data on a SD memory card. DORJI DRF1278F WiFi module is employed to transmit wirelessly acquired data to base station to remotely monitor, in real time, the principal vehicle parameters; WiFi module, a transceiver with LoRa modulation at 433MHz, is based on SX1278 IC provided by Semtech Corporation. Two DORJI DRF1278F modules are used, one installed on vehicle and interfaced with the Nucleo board for data transmission and the other connected to a further Nucleo board, communicating via RS232 with a PC, as receiver at the base station where data are processed and displayed to the technicians. In the next paragraph, the used modules and sensors are illustrated in detail.

## IV. FEATURES OF USED DEVICES AND SENSORS, RELATED FUNCTIONING

The realized telemetry system is composed of different modules, devices and sensors; the technical features and circuital schemes of each employed sensor or electronic module are reported below, besides the connections between different sections of implemented system.

### ✓ ***STM X-Nucleo–F411RE development board***

The STM Nucleo F411RE development board is the central unit of realized telemetry system [18]. The board is provided of connectors (ST Morpho highlitghted in red and Arduino UNO Revision 3 connectors in yellow in Figure 9a), that can be used to expand functionalities of the developing system by connecting very easily external hardware. The Morpho connectors consist of male pins accessibles both from top and bottom of STM board and allow access to all I/O STM microcontroller pins, so ensuring a simplifycation of hardware implementation. In this research work, the Sparkfun CAN-BUS and DORJI WiFi radio module represent the external hardware connected to STM Nucleo board. The STM32F411RET6 microcontroller embedded on the STM Nucleo board, highlighted in Figure 9, is based on the ARM 32-bit Cortex®-M4 microprocessor with a working frequency high up to 100MHz.

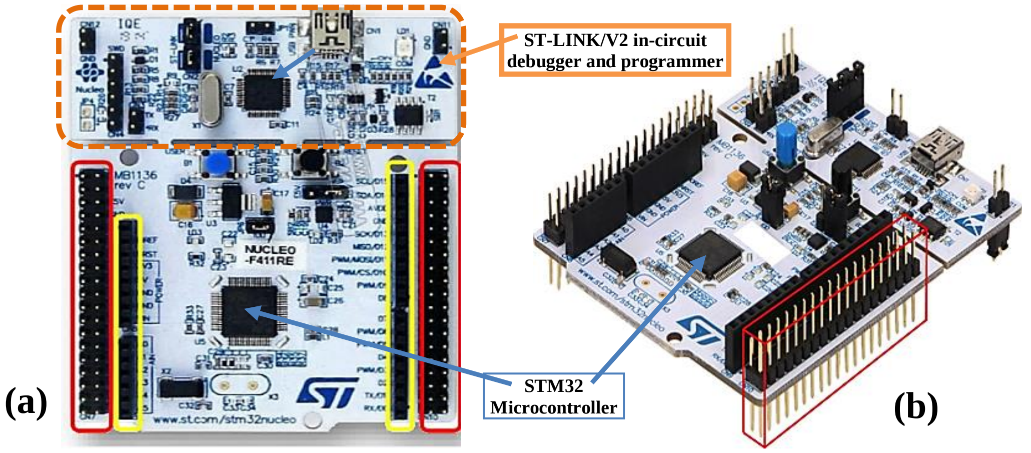

Figure 9. View of the STM32 Nucleo 64-pins board (a) and its lateral view with indication in red of pins-header for the connections with the expansion boards (b).

The microcontroller incorporates high-speed embedded memories (512kB of flash memory and 128kB SRAM), an extensive range of enhanced I/O pins (50 GPIO), a 12 bit ADC with 16 input channels and also provides standard and advanced communication interfaces (namely *I$^2$C*, *SPI*, *USART*, *USB*, *I$^2$S* and *SDIO*). As shown in Figure 9, the STM Nucleo development board is divided in two parts; the first consists of *ST-LINK/V2* in-circuit debugger and programmer with a JTAG/serial wire debugging (SWD) interfaces, whereas, the second part (below) is the main section with embedded the STM microcontroller, different electronic components useful for its proper functioning and Morpho and Arduino UNO Rev3 connectors. Two push buttons, *B1 user* and *B2 reset*, different leds (for USB communication, power and user signaling) are also present on board. In addition, ST-LINK part can be cut out, after the programming phase, to reduce the board size; in this case, the remaining MCU part can only be powered by external $V_{IN}$ through the STM Morpho or Arduino connectors.

STM Nucleo board can be fed through USB connection or by external power supply ranging from 3.3V to 12V; in this work, an external supply voltage of 9V, applied to $V_{IN}$ pin, is used. Relatively to firmware development, it is performed on *MBED* development platform which allows the firmware programming totally on-line without software installation on PC; after the firmware compilation, the output executable file is downloaded by the on-line development environment and installed in the STM microcontroller through USB connection.

### ✓ *Sparkfun CAN-BUS module*

The Sparkfun CAN-BUS module, shown in Figure 10, performs two important tasks, the interfacing between the engine control unit and STM Nucleo board for acquisition of data, provided by Hall sensors and NTC thermistor, and the storing of all detected data on a SD memory card. Furthermore the CAN module allows the vehicle tracking through GPS system;

it presents strong immunity to electromagnetic noise, a important feature in automotive applications [19] [20] [21] and, to further strengthen this feature, twister-pair cables were used.

CAN module operation is based on the MCP2551 and MCP2515 ICs, embedded on board and highlighted in Figure 10a; these ICs allow the communication with the STM Nucleo board through SPI protocol. MCP2515 IC implements the SPI interface, whereas, MCP2551 acts as interface between the MCP2551 and physical bus of the engine control unit for the data reading/writing operations [22]. Figure 10b reports the circuital sections employed for the reading/writing operations on SD memory card. Close to the micro-SD slot (named *usd-socket*), a not-inverting six channels 74HC4050 buffer is mounted; it reduces the $V_{IH}$ voltage values present to its six input channels (1A - 6A) to voltage values $V_{OH}$ for reading/writing operations on SD memory card (3.3V). The three outputs (1Y, 2Y, 3Y) for SPI communication are connected to the *CS*, *DI* and *SCK* inputs of the micro-SD slot.

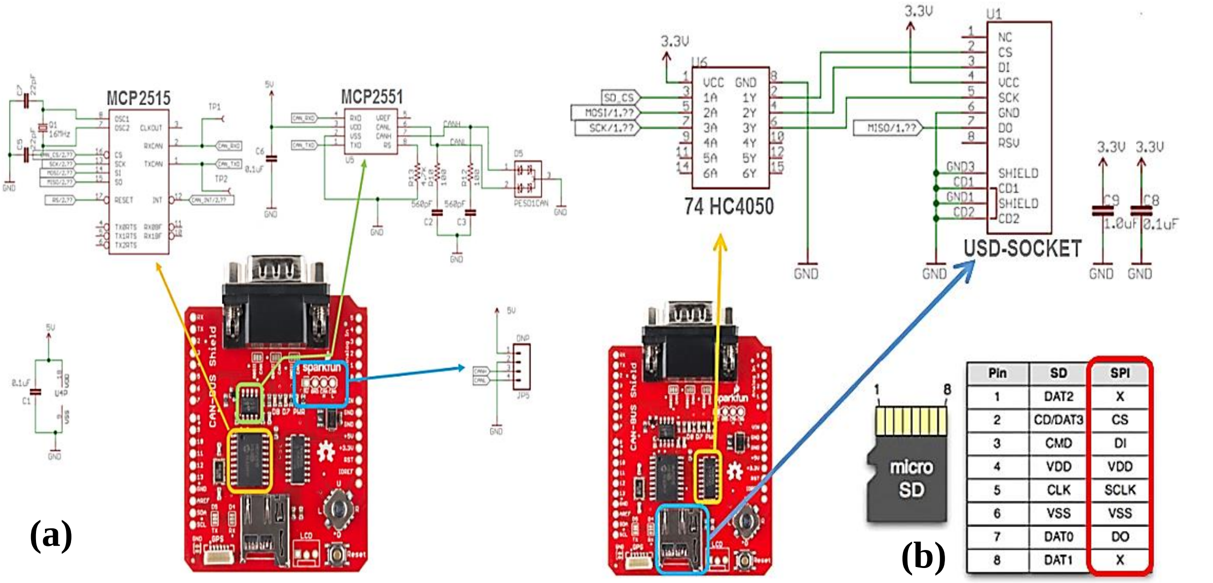

| Pin | SD | SPI |
|---|---|---|
| 1 | DAT2 | X |
| 2 | CD/DAT3 | CS |
| 3 | CMD | DI |
| 4 | VDD | VDD |
| 5 | CLK | SCLK |
| 6 | VSS | VSS |
| 7 | DAT0 | DO |
| 8 | DAT1 | X |

Figure 10. Circuital scheme of SPARKFUN electronic board for the communication by CAN protocol (a), circuital sections employed in writing/reading operations on SD memory card; pins name of SD card, for communication via SPI interface, highlighted in red rectangle (b).

### ✓ *LM35 temperature sensor*

Temperature values to detect into the engine compartment of vehicle range from 15°C to 120°C with a resolution of at least 1C°; LM35 sensor represents an ideal choice thanks to its specifications, namely an output voltage proportional to temperature (sensitivity of 10mV/°C), accuracy of ±¼°C at room temperature and ±¾°C over a full [−55 ÷ 150]°C range and a low output impedance whereas a precise calibration makes the sensor’s interfacing to readout or control circuitry especially easy. In this automotive application, it is expected that the sensor output voltage changes from 0.15V to 1.2V as function of detected temperature (from 15°C to

120°C). The STM32 microcontroller, powered to 3.3V, is provided of an ADC with 12 bit resolution; therefore, the voltage amplitude $q$ of each quantization interval is given by the relation: $q = 3.3/2^{12} = 8*10^{-4}$V = 0.8mV whereas the number of quantization intervals is given by: $\Delta V_{OUT}/q$ = 1312, with $\Delta V_{OUT} = 1.2V – 0.15V$ = 1.05V; hence the temperature resolution is 105°C/1312 = 0.08°C. The four LM35 sensors are connected to ADC input by means of the ST HCF4051 multiplexer, able to select, by a proper digital addressing, desired LM35 sensor for voltage value acquisition. Furthermore, for each temperature sensor, a capacitor of 1µF was used for improving the Sample & Hold operation and reducing the noise contribution.

✓ ***IXTHUS PZ-12-A-75P linear potentiometers***

Linear potentiometers are used for quantifying the suspensions extension during the vehicle motion, thus monitoring its stability in order to adjust eventual functional asymmetries. The excursion to detect is in the range of ±30mm (30mm compression and 30mm extension, with 0.1mm of resolution). The *IXTHUS PZ-12-A-75P* linear potentiometer, shown in Figure 11a, has an optimum mechanical reliability, key factor in environments with particularly adverse conditions, and IP65 certification related to resistance to dust and water [23]. Located close to vehicle suspensions, the potentiometers are provided, in the upper, of a self-aligning spherical joint which guarantees the optimal position for the extension. Used supply voltage is 3.3V and the output voltage is connected to the ADC input of the STM Nucleo board. With a maximum extension of 75mm, potentiometer provides an output voltage of 3.3V, instead at the minimum extension, 0V. As shown in Figure 11b, the potentiometer, in rest conditions, has a portion of the piston (37 mm) in protrusion, so it is possible to detect also the suspensions' contractions. Considering a maximum extension of 60mm, the output voltage $V_{OUT}$ of each potentiometer varies from 0 to 2.64V; being the quantization interval amplitude $q = 3.3V/2^{12}$ = 0.8mV (12 bit ADC resolution), and $\Delta V_{OUT}/q$ = 3300, the obtained resolution is 60 mm/3300 = 0.02 mm.

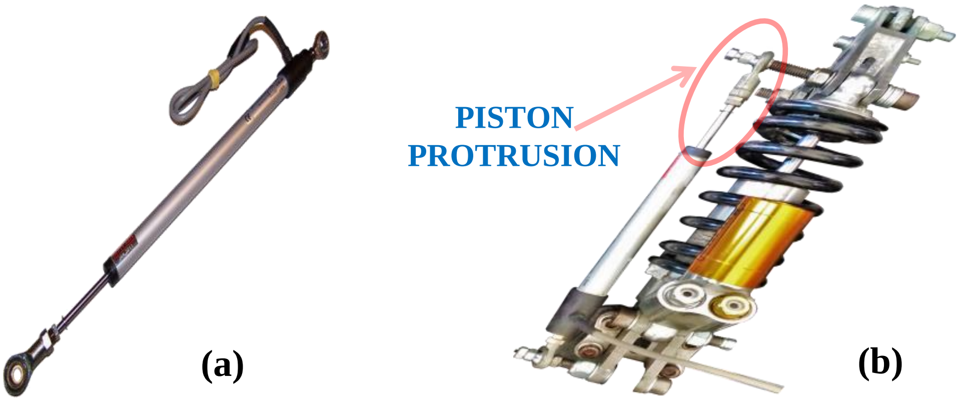

Figure 11. Analog IXTHUS potentiometer used to measure the suspension extension (a) and the sensor mounted on the vehicle suspension (b).

✓ ***HONDA 37870-MAT-E01 Thermistor***

HONDA 37870-MAT-E01 thermistor is employed for monitoring the cooling liquid temperature; it is a 440Ω NTC sensor typology with a resistance value of 440Ω at 25°C which decreases with temperature increasing. The thermistor is connected to the engine control unit, thus connection with Nucleo board takes place by exploiting the Sparkfun CAN-BUS module.

✓ ***CHERRY MEXICO GS1001 Hall effect velocity sensor***

The operation of CHERRY GS1001 digital sensor is based on the Hall effect, able to detect presence of a magnetized metal object, thus providing an output voltage signal proportional to the magnetic field intensity. In the realized telemetry system, Hall effect sensor is located close to a phonic wheel attached to the vehicle wheel, as shown in Figure 12a; by detecting the teeth presence/absence of phonic wheel during its rotation, it is possible to get the rotation speed. The sensor output signal consist of a square wave assuming high logic level (5V) in corrispondence of tooth passing and low logic level (0V) in the section between a tooth and the next (Figure 12b). Therefore, by measuring the square wave period, it is possible to obtain the vehicle speed (range of interest from 0 to 200 km/h); the CHERRY GS1001 sensor has a maximum detection frequency of 15kHz, therefore fully satisfies specifications [24]. Sensor output is connected to the engine control unit in order to convert teeth number passing in front of Hall sensor per second, in vehicle speed value (km/h). In this way, STM Nucleo board receives, through the Sparkfun CAN module, directly the km/h value related to vehicle speed.

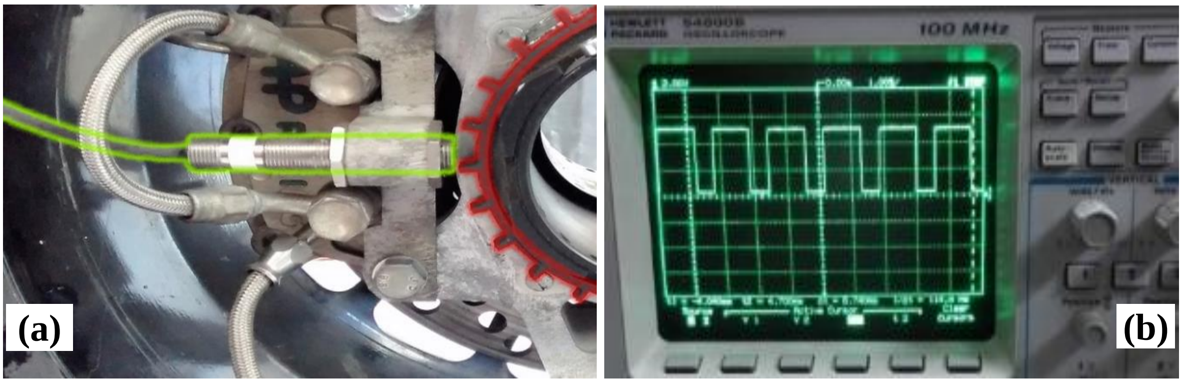

Figure 12. Hall sensor positioned in front of the phonic wheel to detect its rotation speed (a) and square wave provided by sensor and acquired by the Tektronix oscilloscpe (b).

✓ ***MPU-6050 Gyroscope/accelerometer***

The *InvenSense MPU-6050* gyroscope/accelerometer, shown in Figure 13a mounted on the interfacing board used in this research work, is mostly employed by smartphone and tablet manufacturers due to the enormous value it adds to the end user experience. For smartphones, it is used for phone control, enhanced gaming, augmented reality, panoramic photo capture and viewing, and pedestrian/vehicle navigation. In our automotive application, the *MPU-6050* sensor is used, located at the center of vehicle, to characterize vehicle motion relatively to pith, roll and yawing, thus allowing to analyze data related to acceleration and inclination angles. In Figure 13b, the circuital scheme of interfacing board is reported; MPU-6050 sensor requires 3.3V for proper functioning obtained by MIC5205 voltage regulator (5V/3.3V). The gyroscope/accelerometer integrates 6-axis *MotionTracking* device that combines a 3 axis MEMS (*Micro Electro-Mechanical System*) gyroscope, a 3 axis MEMS accelerometer and DMP (*Digital Motion Processor*) to process algorithms for movement tracking up to 9 axis.

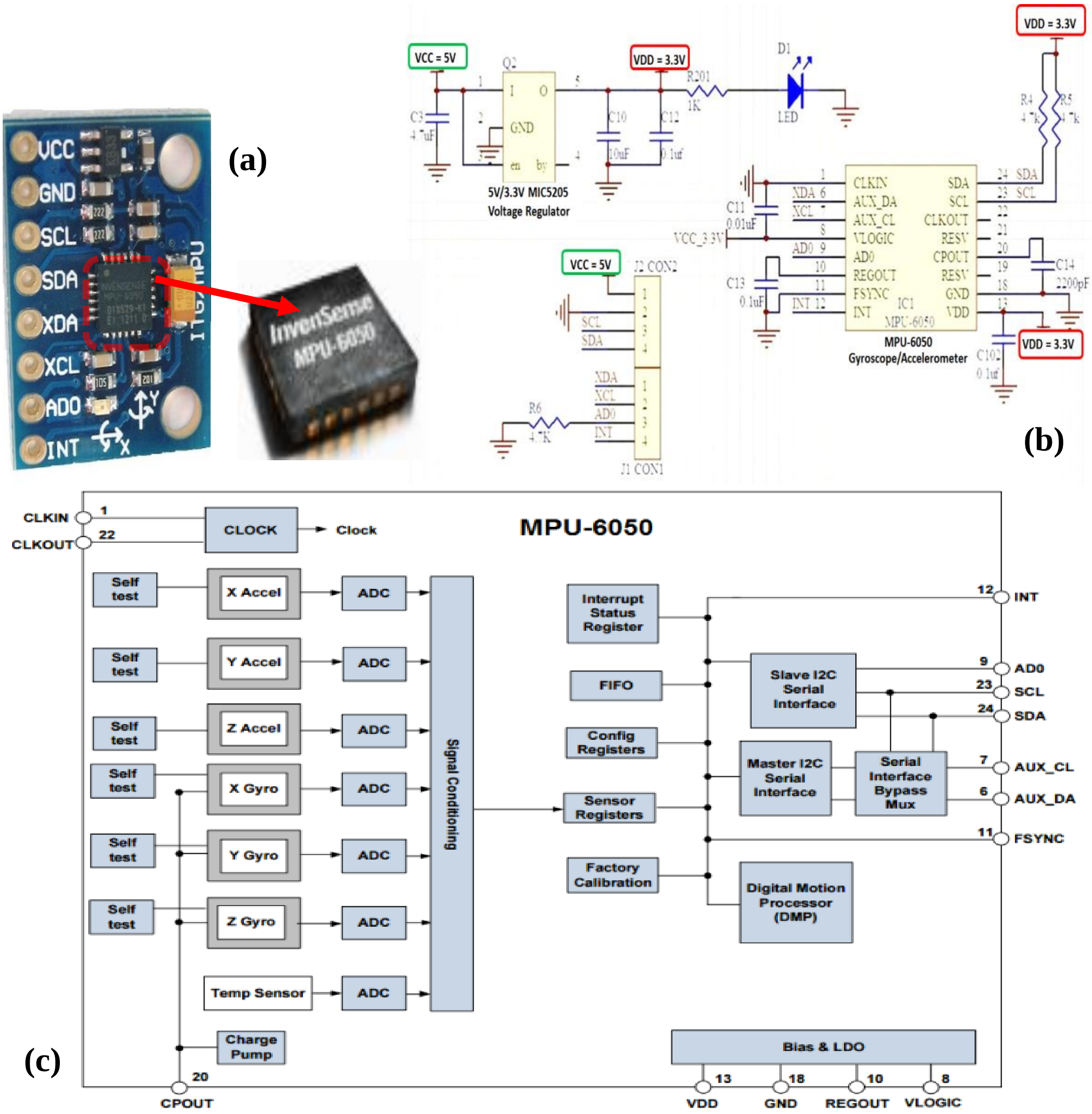

Figure 13. Interfacing board with integrated the MPU6050 gyroscope/accelerometer sensor (a), circuital scheme of the breakout board with the MIC5105 voltage regulator (b) and the inner block diagram of the MPU-6050 gyroscope/accelerometer (c).

As reported in the MPU-6050 inner block diagram of Figure 13c, the sensor features three 16-bit ADCs for digitizing the gyroscope outputs and three 16-bit ADCs for the accelerometer outputs; a further ADC is used for reading of on-chip temperature sensor [25]. For accurate tracking of both fast and slow motions, it is possible to set, in the programming firmware, different gyroscope sensitivity ranges (± 250, ± 500, ± 1000, ± 2000 degree/sec). For the accelerometer, the settable ranges are the following: ± 2g, ± 4g, ± 8g and ± 16g. In the developed firmware, setted values for gyroscope and accelerometer were ± 500 degree/sec and ± 4g respectively, an ideal choice in order to have a precise and accurate vehicle motion tracking. The MPU-6050 sensor features different registers to store acquired data as shown in Figure 13c; communication with all registers is performed using either I$^2$C protocol (used also, in this case, for communicating with ST Nucleo board) or SPI protocol (used with other MPU sensor modules). A $V_{LOGIC}$ reference pin (in addition to analog supply pin $V_{DD}$), can be used to set logic levels of I$^2$C interface. In Figure 14, the connection between the *InvenSense MPU-6050* gyroscope/accelerometer sensor and the STM Nucleo board is shown; for the communication by means of the I$^2$C interface, the STM Nucleo PB8 and PB9 pins were used.

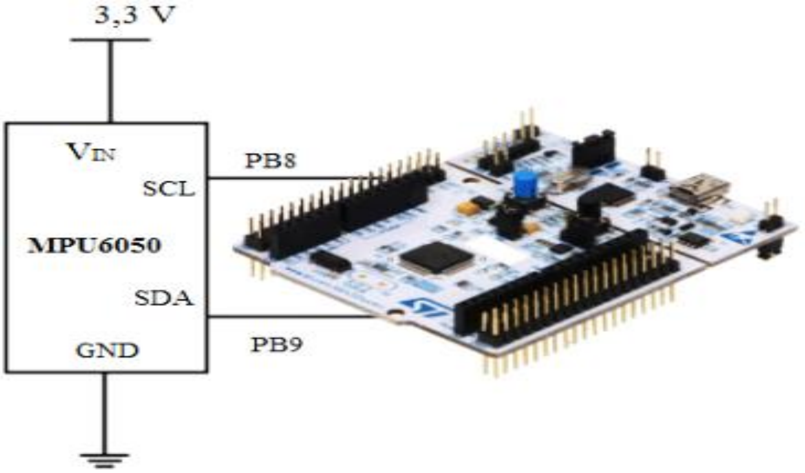

Figure 14. Connection, through the PB8 and PB9 input pins of ST Nucleo borad, between the ST Nucleo development board and the MPU6050 gyroscope/accelerometer sensor.

✓ ***DORJI DRF1278F WiFi transceiver module.***

The DRF1278F Wi-Fi radio module, used for data transmitting to the base station, is shown in Figure 15 soldered on an adapting board realized for easy interfacing with ST Nucleo board and for connecting an external antenna. The module employs the SX1278 IC transceiver from Semtech Corporation and is provided of a thin SMD crystal and needed components for the antenna matching circuit. DRF1278F module operates at 1.8V - 3.6V, exploits *LoRa* (Long Range) modulation [26, 27] with the *Chirp Spread Spectrum* (*CSS)* modulation method; each bit is spread by a chipping factor and the number of chips per bit is called *spread factor*.

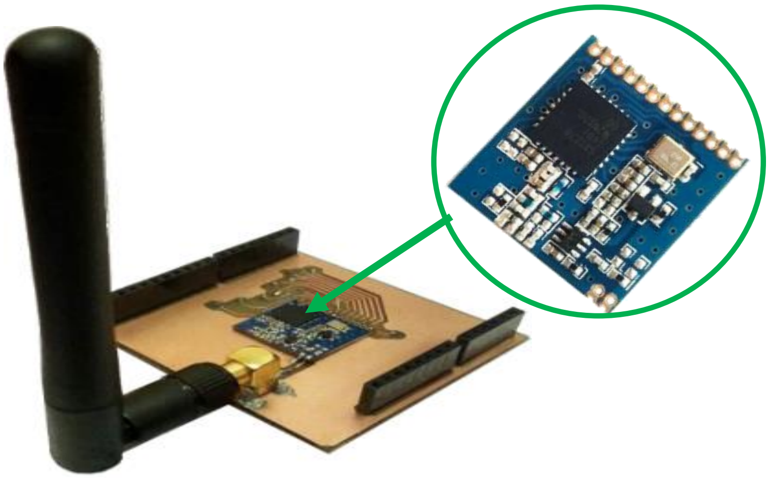

Figure 15. Realized adapting board for interfacing the DRF1278F module with ST Nucleo board and to connect an external antenna.

The generated chirp signal continuously varies in frequency; in this way, timing and frequency offsets between transmitter and receiver are equivalent, thus reducing the complexity of the receiver design [28]. The frequency bandwidth of chirp is equivalent to spectral bandwidth of the signal; obviously, at larger spreading factor, slower data rate corresponds, better receiver sensitivity and consequently longer potential communication range [29]. DRF1278F Wi-Fi radio module is featured by a frequency range of 433MHz and a data rate up to 300 kbps. In Figure 16, an example of four bits (1001) sent with a spreading factor of 7, with the chip pattern for the digital value "1" and that for the digital value "0", is shown.

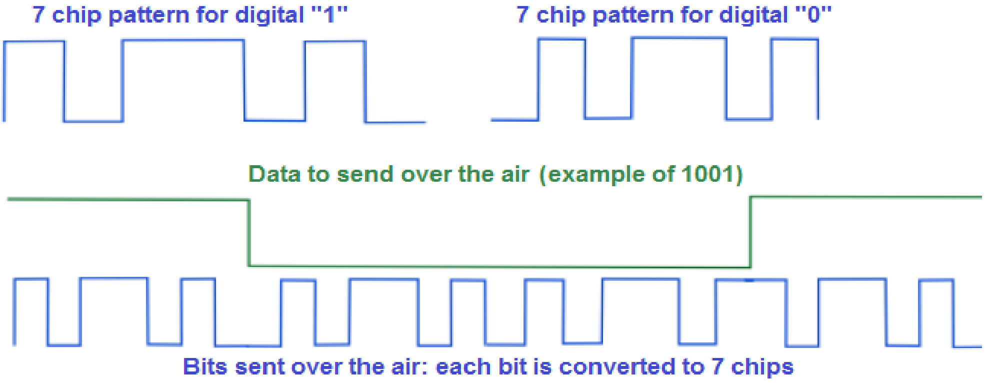
7 chip pattern for digital "1"
7 chip pattern for digital "0"
Data to send over the air (example of 1001)
Bits sent over the air: each bit is converted to 7 chips

Figure 16. Example of sending bits using LoRa modulation with spreading factor equal to 7.

## V. FIRMWARE IMPLEMENTATION IN ARM MBED ENVIRONMENT FOR MONITORING THE FORMULA SAE VEHICLE PARAMETERS

In Figure 17, the flow chart related to the main operations performed by developed firmware is shown: as reported in its first section (Figure 17a), first operations concern the initialization of the Sparkfun CAN-BUS and Wi-Fi modules; if this phase fails, a LED, located in the passenger compartment, is turned on. Then, the initialization operation is repeated and, if error occurs again, LED is turned on intermittently for warning user of modules malfunction. Once carried out modules initialization, data are acquired from both sensors directly connected with ST Nucleo board and through the engine control unit (as shown in Figure 17b). Also in this phase if in the reading operations errors occur, the user is alerted by related LED flashing.

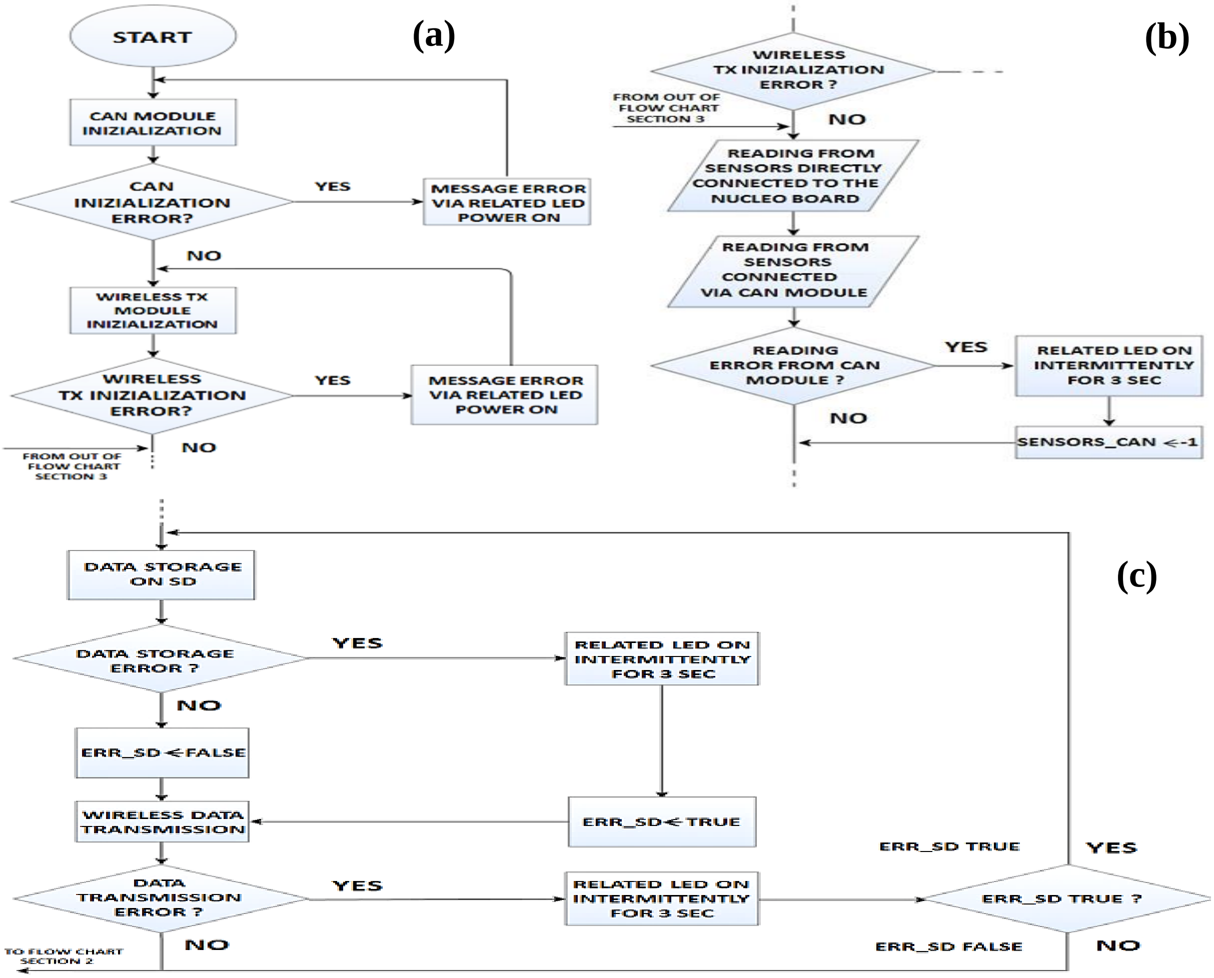
(a)
START
CAN MODULE INIZIALIZATION
CAN INIZIALIZATION ERROR?
YES
MESSAGE ERROR VIA RELATED LED POWER ON
NO
WIRELESS TX MODULE INIZIALIZATION
WIRELESS TX INIZIALIZATION ERROR?
YES
MESSAGE ERROR VIA RELATED LED POWER ON
NO
FROM OUT OF FLOW CHART SECTION 3
(b)
WIRELESS TX INIZIALIZATION ERROR ?
FROM OUT OF FLOW CHART SECTION 3
NO
READING FROM SENSORS DIRECTLY CONNECTED TO THE NUCLEO BOARD
READING FROM SENSORS CONNECTED VIA CAN MODULE
READING ERROR FROM CAN MODULE ?
YES
RELATED LED ON INTERMITTENTLY FOR 3 SEC
SENSORS_CAN <-1
NO
(c)
DATA STORAGE ON SD
DATA STORAGE ERROR ?
YES
RELATED LED ON INTERMITTENTLY FOR 3 SEC
NO
ERR_SD <-FALSE
ERR_SD<-TRUE
WIRELESS DATA TRANSMISSION
DATA TRANSMISSION ERROR ?
YES
RELATED LED ON INTERMITTENTLY FOR 3 SEC
ERR_SD TRUE ?
ERR_SD TRUE
YES
ERR_SD FALSE
NO
NO
TO FLOW CHART SECTION 2

Figure 17. Flow chart divided in three sections; the first related to CAN and WiFi modules initialization (a), second section to reading operations from all sensors (b), the third related to data storage on SD memory card and to data sending, via WiFi module, to the base station (c).

The communication between STM Nucleo board and CAN module is verified by controlling cardinality of exchanged data; if zero, then it means errors presence and system warns the user turning on an intermittent LED (related to CAN module). Then, as visible in the flow chart, different controls are performed by firmware on the writing operation on SD memory card and on wireless transmission. If writing operation is successful and wireless transmission fails, then system proceeds equally with cycle completion because a copy of acquired data has been correctly stored. On the contrary, if writing operation on SD presents errors but Wi-Fi module operates correclty, data are equally sent to base station; anyhow all malfunctions are warned to user by means of LEDs, resulting a particularly reliable and stable telemetry system.

The firmware is structured so that all acquired values, related to temperature, car speed, suspensions' extension, acceleration and so on are saved into *TelemetryValues* data structure, implemented for collecting data from all sensors, first to transmit them to the base station. The four LM35 temperature sensors are connected, through the multiplexer, to the PC4 analog pin of the STM Nucleo board; developed firmware, before to acquire analog value from sensors, manages the multiplexer for selecting, by using proper logic adressing, desired LM35 sensor for the reading operation [30]. Implemented *mux_sel()* function (Figure 19) allows, through the integer parameter *n*, to select the appropriate sensor as shown in table of Figure 18.

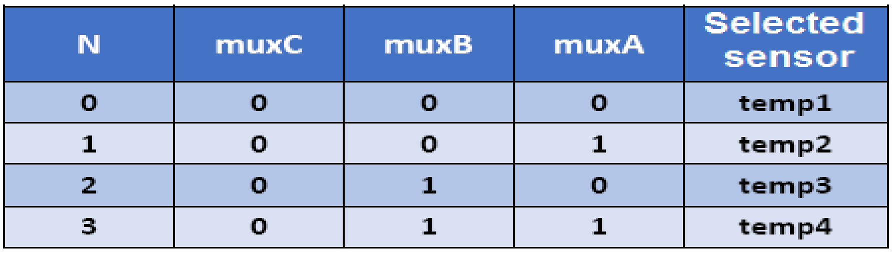

| N | muxC | muxB | muxA | Selected sensor |
|---|---|---|---|---|
| 0 | 0 | 0 | 0 | temp1 |
| 1 | 0 | 0 | 1 | temp2 |
| 2 | 0 | 1 | 0 | temp3 |
| 3 | 0 | 1 | 1 | temp4 |

Figure 18. Table with the index "N" used in the firmware to select, through the multiplexer, the desired LM35 sensor for temperature value reading.

The reading operation is performed by the *read_temp()* function, shown in Figure 19b; it returns the temperature value expressed in °C. In the firmware section reported in Figure 19c, the acquired temperature values are assigned to the *v.temp1*, *v.temp2*, *v.temp3 and 4* variables of the *TelemetryValues* structure, to be stored and then sent wirelessly to the base station.

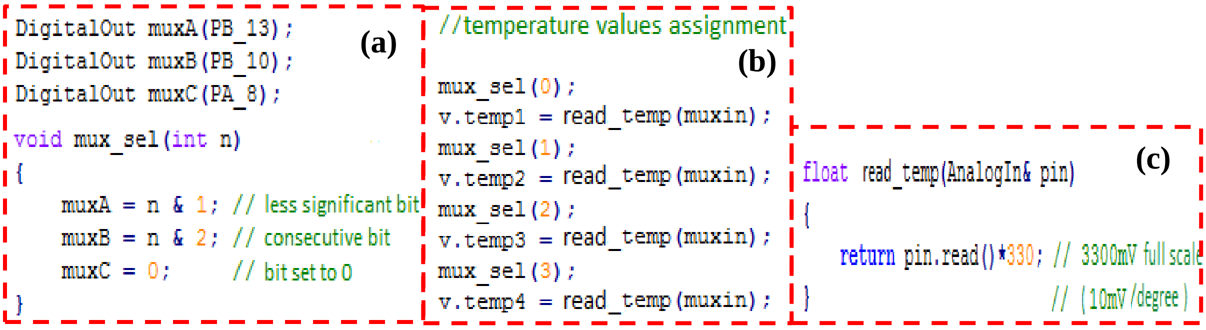

```
DigitalOut muxA(PB_13);
DigitalOut muxB(PB_10);
DigitalOut muxC(PA_8);

void mux_sel(int n)
{
    muxA = n & 1; // less significant bit
    muxB = n & 2; // consecutive bit
    muxC = 0;     // bit set to 0
}
```

```
//temperature values assignment

mux_sel(0);
v.temp1 = read_temp(muxin);
mux_sel(1);
v.temp2 = read_temp(muxin);
mux_sel(2);
v.temp3 = read_temp(muxin);
mux_sel(3);
v.temp4 = read_temp(muxin);
```

```
float read_temp(AnalogIn& pin)
{
    return pin.read()*330; // 3300mV full scale
}                          // (10mV/degree)
```

Figure 19. Firmware sections related to the LM35 sensor selection through the multiplexer (a), to the temperature value reading and conversion phases (b) and to value assignment in the proper field of the TelemetryValues structure (c).

In Figure 20, firmware sections related to the reading operation from *IXTHUS* potentiometers are shown; Figure 20a reports the variables declarations, with the four potentiometers directly connected to PA1, PA4, PB0 and PC1 pins of STM Nucleo board, corresponding to rear left, rear right, front left and front right suspensions respectively. Also in this case, as well as for temperature sensors, the potentiometers provide an analog value as output; therefore, a formula, to convert the acquired voltage value in the extension value, expressed in mm, is used (Figure 20b). The implemented function returns a value equal to 0 when potentiometer is at rest and positive values when extended. After the reading operation, the acquired values are assigned to *TelemetryValues* structure (Figure 20c), to be stored and then sent to base station.

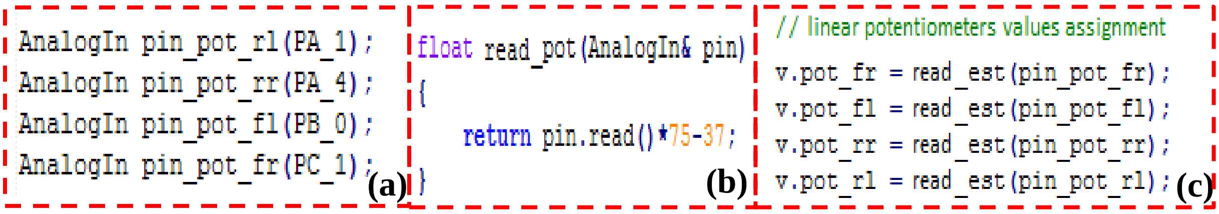

```
AnalogIn pin_pot_rl(PA_1);
AnalogIn pin_pot_rr(PA_4);
AnalogIn pin_pot_fl(PB_0);
AnalogIn pin_pot_fr(PC_1);
```

```
float read_pot(AnalogIn& pin)
{
    return pin.read()*75-37;
}
```

```
// linear potentiometers values assignment
v.pot_fr = read_est(pin_pot_fr);
v.pot_fl = read_est(pin_pot_fl);
v.pot_rr = read_est(pin_pot_rr);
v.pot_rl = read_est(pin_pot_rl);
```

Figure 20. Implemented firmware for acquisition and processing of the signals provided from linear potentiometers; firmware section related to variables declaration (a), to conversion (in mm) of detected value and offset removal (b) and to *TelemetryValues structure* assignment (c).

The management of the MPU6050 gyroscope/accelerometer sensor is performed by firmware sections reported in Figure 21a; the communication with sensor is performed by $I^2C$ protocol and all needed functions and libraries are available on *www.mbed.com* webpage (online platform provided from *STMicroelectronics* for firmware programming). Developed firmware concerns the implementation of the intialization, calibration and data acquisition functions. As shown in Figure 21a, if the function *whoAmI* is true, then sensor is correcly connected and calibration and initialization operations are performed; on the contrary, if the *whoAmI* returns false, a LED is turned on for alerting sensor malfunctioning. Data provided from MPU6050 sensor are managed by the *getA*, *getG* functions which return the values, along the three axes, related to the car acceleration, yaw, pitch and roll angle. Finally, the data are assigned to the *TelemetryValues* database (Figure 21b). In this phase, the values assignment is carried out only if sensor is correcly connected; if the *mpu6050.ok()* function is true (sensor correctly connected), then firmware proceeds to assign acquired values to *TelemetryValues* data structure, on the contrary, the variables, in the data structure, will assume the value *-1* (see Figure 21b).

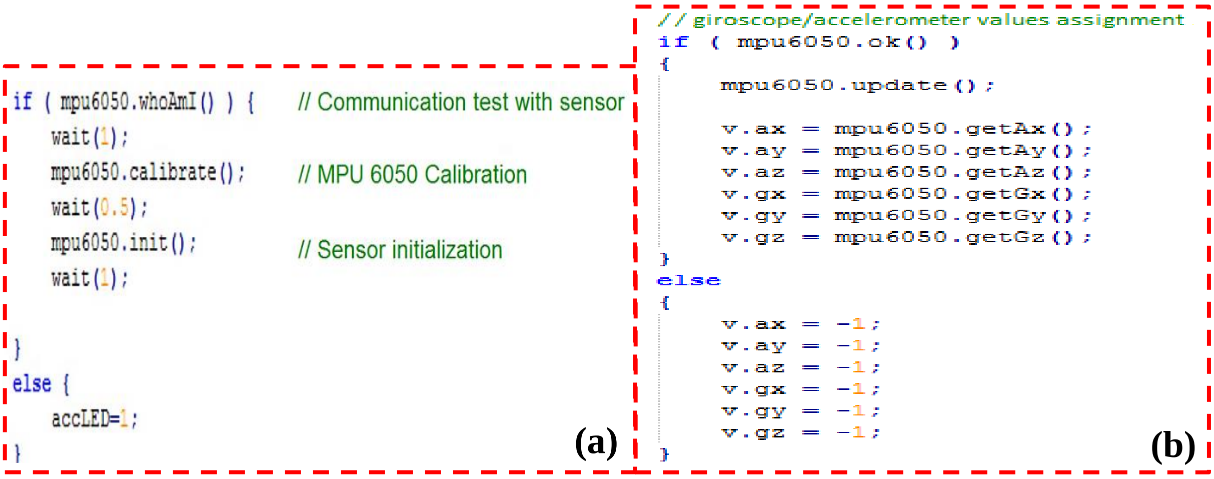

```
if ( mpu6050.whoAmI() ) {      // Communication test with sensor
    wait(1);
    mpu6050.calibrate();       // MPU 6050 Calibration
    wait(0.5);
    mpu6050.init();            // Sensor initialization
    wait(1);

}
else {
    accLED=1;
}
```

```
// giroscope/accelerometer values assignment
if ( mpu6050.ok() )
{
    mpu6050.update();

    v.ax = mpu6050.getAx();
    v.ay = mpu6050.getAy();
    v.az = mpu6050.getAz();
    v.gx = mpu6050.getGx();
    v.gy = mpu6050.getGy();
    v.gz = mpu6050.getGz();
}
else
{
    v.ax = -1;
    v.ay = -1;
    v.az = -1;
    v.gx = -1;
    v.gy = -1;
    v.gz = -1;
}
```

Figure 21. Firmware sections related to the acquisition/processing of data provided from the gyroscope/accelerometer sensor (a) and to TelemetryValues structure assignment (b).

The STM Nucleo board acquires data from sensors directly connected to the engine control unit (Hall effect sensors and the NTC thermistor) through the Sparkfun CAN-BUS module. Firmware implemented for CAN module management is divided into two main sections: one related to the interfacing between the CAN module and engine control unit (for sensors reading) and the other one related to data storage on the SD memory card. In the first section, the firmware performs a control on CAN module initialization (Figure 22a): the *canInit_ok* boolean variable assumes logic value 1 if the initialization has correctly occurred, otherwise a LED is turned on. Once performed the initialization operation, the *nframe* boolean variable is used to check the correct communication between the CAN module and engine control unit (Figure 22b); if it is true, the reading operations from Hall sensors and NTC thermistor are performed, on the contrary, an intermittent LED warns of the error and the value *-1* is assigned.

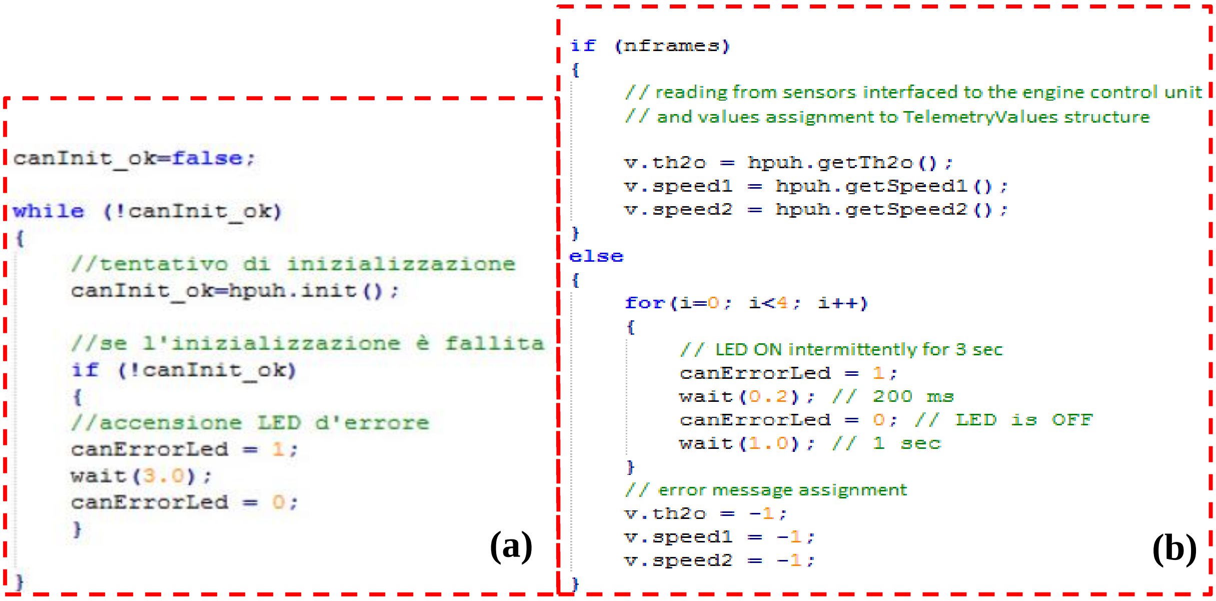

```
canInit_ok=false;

while (!canInit_ok)
{
    //tentativo di inizializzazione
    canInit_ok=hpuh.init();

    //se l'inizializzazione è fallita
    if (!canInit_ok)
    {
    //accensione LED d'errore
    canErrorLed = 1;
    wait(3.0);
    canErrorLed = 0;
    }
}
```

```
if (nframes)
{
    // reading from sensors interfaced to the engine control unit
    // and values assignment to TelemetryValues structure

    v.th2o = hpuh.getTh2o();
    v.speed1 = hpuh.getSpeed1();
    v.speed2 = hpuh.getSpeed2();
}
else
{
    for(i=0; i<4; i++)
    {
        // LED ON intermittently for 3 sec
        canErrorLed = 1;
        wait(0.2); // 200 ms
        canErrorLed = 0; // LED is OFF
        wait(1.0); // 1 sec
    }
    // error message assignment
    v.th2o = -1;
    v.speed1 = -1;
    v.speed2 = -1;
}
```

Figure 22. Firmware sections related to the CAN module initialization (a) and to data acquisition from the Hall sensors and NTC thermistor (b).

Once completed reading operations from all sensors, both those connected directly with ST Nucleo board and through CAN module, data are stored on SD memory card. The operation is carried out by implemented *save_sd()* function (Figure 23); all values of the *TelemetryValues* structure, containing all data provided from sensors, are converted into a string form and written on the SD memory card. Furthermore, a check of the writing operation is carried out; if errors occur, the related LED, as previously described, is turned on for warning the user.

The last part of this paragraph concerns the developed firmware for DRF1278F Wi-Fi module management; it is based on libraries, availables on *www.mbed.com*, containing all functions for data transmission and reception. First operation regards the WiFi module initialization and parameters setting for the correct communication with the STM Nucleo board (see Figure 24).

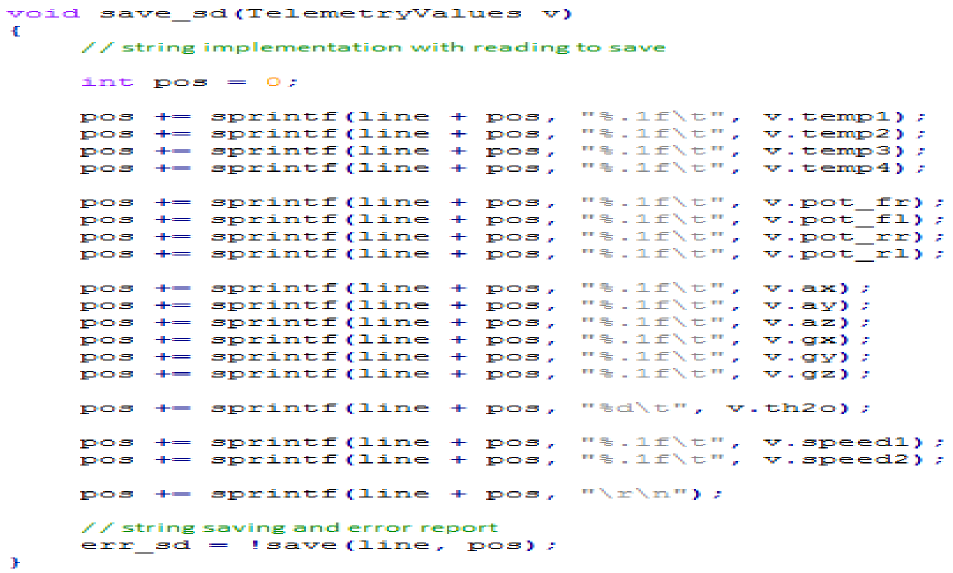

```
void save_sd(TelemetryValues v)
{
        // string implementation with reading to save

        int pos = 0;

        pos += sprintf(line + pos, "%.1f\t", v.temp1);
        pos += sprintf(line + pos, "%.1f\t", v.temp2);
        pos += sprintf(line + pos, "%.1f\t", v.temp3);
        pos += sprintf(line + pos, "%.1f\t", v.temp4);

        pos += sprintf(line + pos, "%.1f\t", v.pot_fr);
        pos += sprintf(line + pos, "%.1f\t", v.pot_fl);
        pos += sprintf(line + pos, "%.1f\t", v.pot_rr);
        pos += sprintf(line + pos, "%.1f\t", v.pot_rl);

        pos += sprintf(line + pos, "%.1f\t", v.ax);
        pos += sprintf(line + pos, "%.1f\t", v.ay);
        pos += sprintf(line + pos, "%.1f\t", v.az);
        pos += sprintf(line + pos, "%.1f\t", v.gx);
        pos += sprintf(line + pos, "%.1f\t", v.gy);
        pos += sprintf(line + pos, "%.1f\t", v.gz);

        pos += sprintf(line + pos, "%d\t", v.th2o);

        pos += sprintf(line + pos, "%.1f\t", v.speed1);
        pos += sprintf(line + pos, "%.1f\t", v.speed2);

        pos += sprintf(line + pos, "\r\n");

        // string saving and error report
        err_sd = !save(line, pos);
}
```

Figure 23. Firmware section related to data storage on SD memory card: all data acquired from sensors are converted into string form and stored on the SD memory card.

The implemented function *lora_init()* checks the WiFi module connection through a reading operation from a particular register of the module; if the returned value is 0, then module is not connected, otherwise firmware proceeds with the parameters setting. At the end of the initialization phase, DRF1278F Wi-Fi module is ready for data transmission; the used *lora_send()* function takes as parameter the *TelemetryValues* data structure. The data transmission is carried out in two distinct phases: in the first phase, data are saved into buffers and subsequently, in the second phase, they are effectively sent. In this last phase, if wireless transmission is difficult for any reason, for example it takes a long time, the *OnTxTimeout()* function is automatically invoked to try to solve the problem and to warn the user.

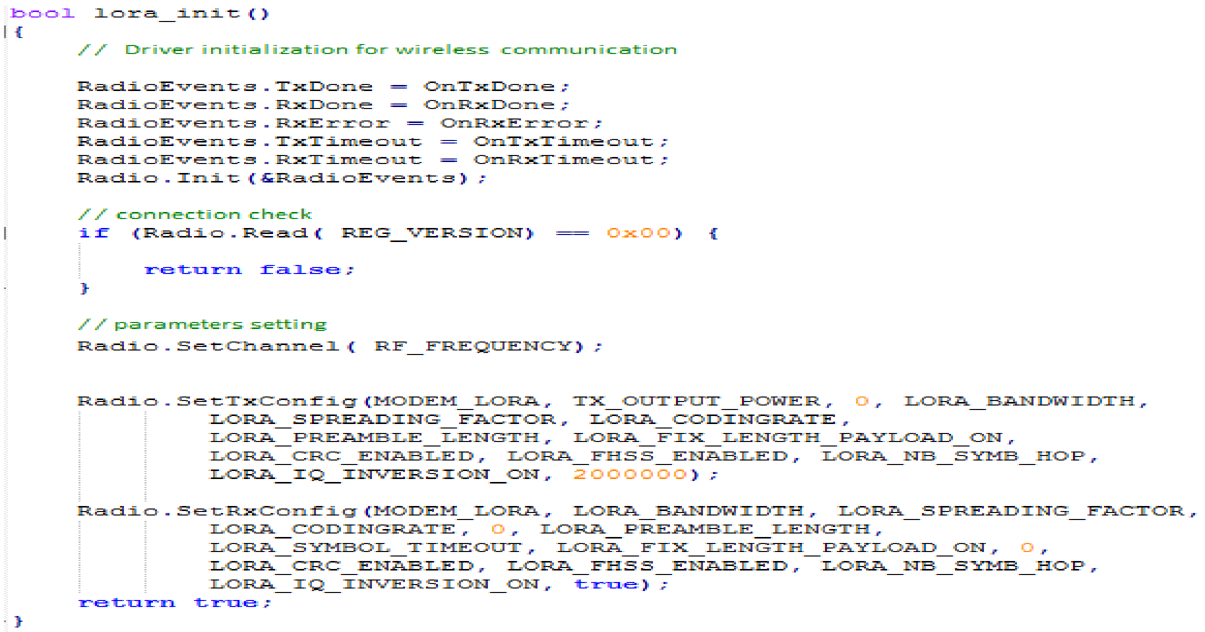

```
bool lora_init()
{
      // Driver initialization for wireless communication

      RadioEvents.TxDone = OnTxDone;
      RadioEvents.RxDone = OnRxDone;
      RadioEvents.RxError = OnRxError;
      RadioEvents.TxTimeout = OnTxTimeout;
      RadioEvents.RxTimeout = OnRxTimeout;
      Radio.Init(&RadioEvents);

      // connection check
      if (Radio.Read( REG_VERSION) == 0x00) {

          return false;
      }

      // parameters setting
      Radio.SetChannel( RF_FREQUENCY);


      Radio.SetTxConfig(MODEM_LORA, TX_OUTPUT_POWER, 0, LORA_BANDWIDTH,
                LORA_SPREADING_FACTOR, LORA_CODINGRATE,
                LORA_PREAMBLE_LENGTH, LORA_FIX_LENGTH_PAYLOAD_ON,
                LORA_CRC_ENABLED, LORA_FHSS_ENABLED, LORA_NB_SYMB_HOP,
                LORA_IQ_INVERSION_ON, 2000000);

      Radio.SetRxConfig(MODEM_LORA, LORA_BANDWIDTH, LORA_SPREADING_FACTOR,
                LORA_CODINGRATE, 0, LORA_PREAMBLE_LENGTH,
                LORA_SYMBOL_TIMEOUT, LORA_FIX_LENGTH_PAYLOAD_ON, 0,
                LORA_CRC_ENABLED, LORA_FHSS_ENABLED, LORA_NB_SYMB_HOP,
                LORA_IQ_INVERSION_ON, true);
      return true;
}
```

Figure 24. Firmware section for WiFi radio module initialization and parameters setting.

On the receiving side, the implemented instructions are shown in Figure 25; DRF1278F Wi-Fi module is initialized through the *lora_init()* function, the same used for the data transmission.

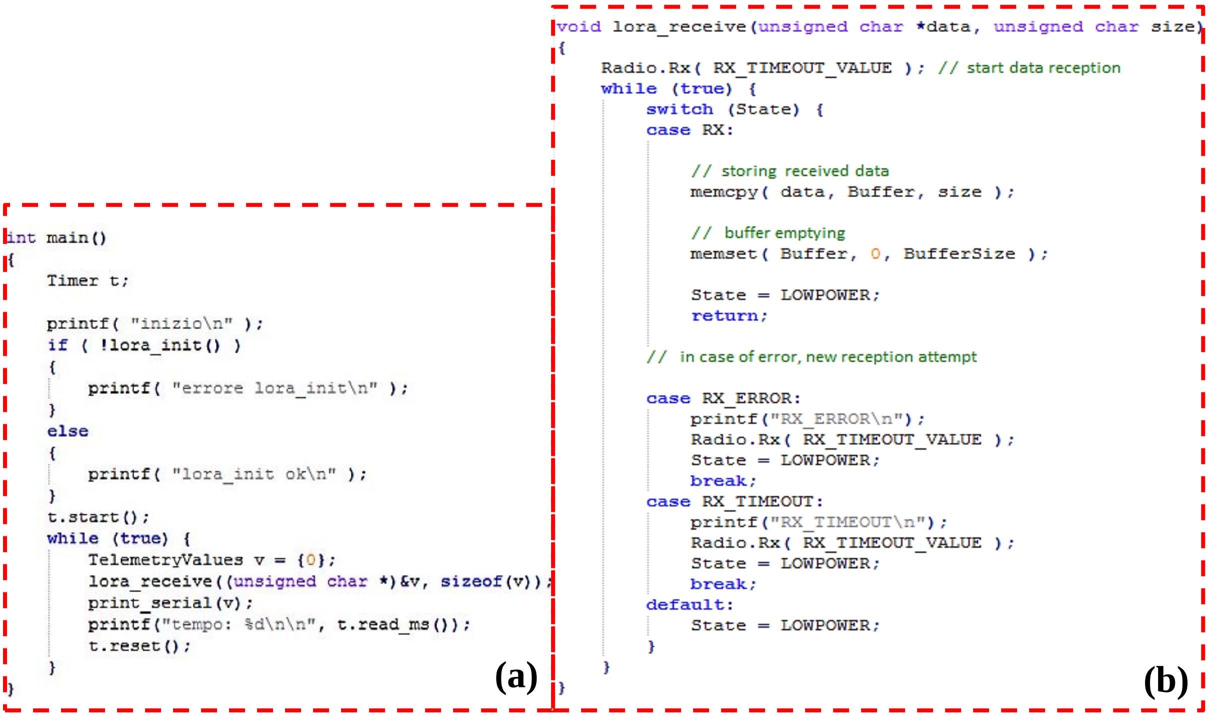

```
int main()
{
    Timer t;

    printf( "inizio\n" );
    if ( !lora_init() )
    {
        printf( "errore lora_init\n" );
    }
    else
    {
        printf( "lora_init ok\n" );
    }
    t.start();
    while (true) {
        TelemetryValues v = {0};
        lora_receive((unsigned char *)&v, sizeof(v));
        print_serial(v);
        printf("tempo: %d\n\n", t.read_ms());
        t.reset();
    }
}
```

```
void lora_receive(unsigned char *data, unsigned char size)
{
    Radio.Rx( RX_TIMEOUT_VALUE ); // start data reception
    while (true) {
        switch (State) {
        case RX:

            // storing received data
            memcpy( data, Buffer, size );

            // buffer emptying
            memset( Buffer, 0, BufferSize );

            State = LOWPOWER;
            return;

        //  in case of error, new reception attempt

        case RX_ERROR:
            printf("RX_ERROR\n");
            Radio.Rx( RX_TIMEOUT_VALUE );
            State = LOWPOWER;
            break;
        case RX_TIMEOUT:
            printf("RX_TIMEOUT\n");
            Radio.Rx( RX_TIMEOUT_VALUE );
            State = LOWPOWER;
            break;
        default:
            State = LOWPOWER;
        }
    }
}
```

Figure 25. Firmware section related to data reception from the base station (a) and to the implemented *lora_receive()* function (b).

By using the *lora_receive()* function, shown in Figure 25b, the transmitted data are received by the base station and subsequently displayed on PC connected, via USB cable, with the ST Nucleo board [31-34]. The *Radio.Rx()* function, used for starting the data reception, is available on the *mbed* webpage in the proper section dedicated to DRF1278F WiFi module with embedded the SX1278 IC transceiver. As shown in Figure 25b, the data correctly received are copied and printed on the PC terminal for the technicians analysis, emptying subsequently the buffer, whereas, if there are errors a new data reception cycle is carried out.

## VI. HARDWARE AND FIRMWARE TESTING OF USED SENSORS AND MODULES BEFORE MOUNTING THE TELEMETRY SYSTEM ON THE VEHICLE

In this paragraph, the different test phases, carried out for verifying the correct operation of each sensor and electronic module employed in the telemetry system, are illustrated. Finally, verification of the proper functioning of the complete realized system, assembled on board the vehiche, will be performed. In Figure 26, the operation test of the IXTHUS potentiometer is shown; the sensor analog output was applied to ADC input pin (PA1) of ST Nucleo board, this last connected to PC, through USB cable, for serial communication. When potentiometer is totally compressed, the extension value 0.0-0.1, provided by the STM Nucleo board as result of the A/D conversion and processing, is printed on PC terminal. For this test, the used conversion formula, implemented in the firmware, doesn’t take into account the protrusion position (potentiometer at rest); therefore, at “0” position corresponds the 0 extension value on PC and not the negative value (-37 mm). On the other hand, when potentiometer is totally extended, i.e. extension of 75mm, the A/D conversion and subsequent processing provides as result the correct value of the potentiometer extension, as shown in Figure 26b.

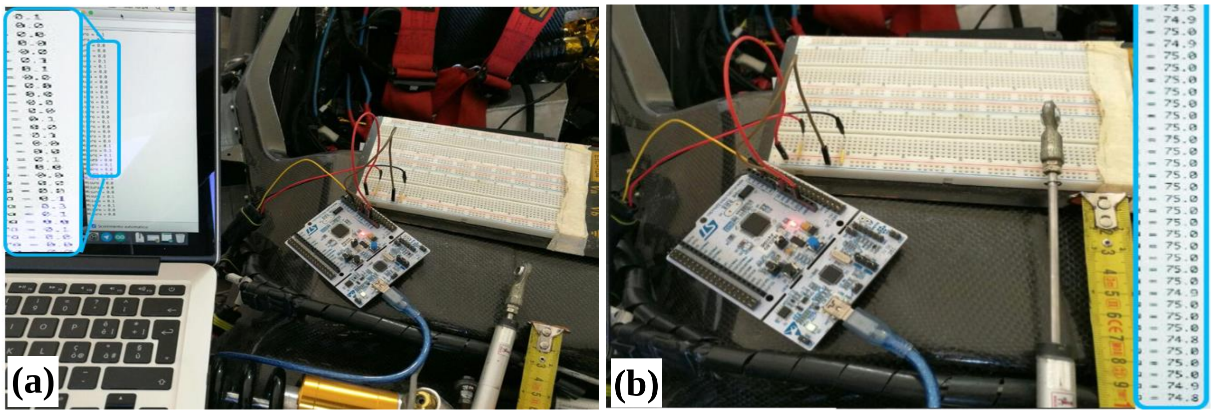

```
- 0.1
- 0.0
- 0.0
- 0.0
- 0.0
- 0.1
- 0.1
- 0.0
- 0.0
- 0.0
- 0.0
- 0.0
- 0.1
- 0.0
- 0.1
- 0.0
- 0.0
- 0.1
- 0.0
- 0.0
- 0.0
- 0.0
- 0.1
- 0.1
- 0.1
- 0.0
- 0.1
- 0.0
- 0.0
```

```
- 73.5
- 74.9
- 75.0
- 74.9
- 75.0
- 75.0
- 75.0
- 75.0
- 75.0
- 75.0
- 75.0
- 75.0
- 75.0
- 75.0
- 75.0
- 75.0
- 75.0
- 75.0
- 75.0
- 75.0
- 75.0
- 75.0
- 75.0
- 75.0
- 74.9
- 75.0
- 75.0
- 75.0
- 74.8
- 75.0
- 75.0
- 75.0
- 74.9
- 74.8
```

Figure 26. Experimental setup for potentiometer operation test; the analog signal provided by sensor is acquired and processed from ST Nucleo board and displayed on PC (0 extention corresponds to 0.0 value (a), by increasing the extention, displayed value rises up to 75mm (b).

Figure 27 is related to the test phase carried out for proper functioning verification of the LM35 temperature sensors; LM35 sensor is connected directly to the PC4 analog input pin of ST Nucleo board and this last, through an USB cable, to PC for data exchange and viewing [35-37]. The detected temperature value, resulting from the A/D conversion and subsequent formula application, as reported in the firmware paragraph, was 25-26°C; the same voltage values provided by LM35 sensor were acquired and visualized by using the Tektronix 2024B oscilloscope (a voltage value of 263mV corresponds to a temperature of ≈ 26°C), so verifying the proper operation of the LM35 sensor and related data acquisition and processing phases.

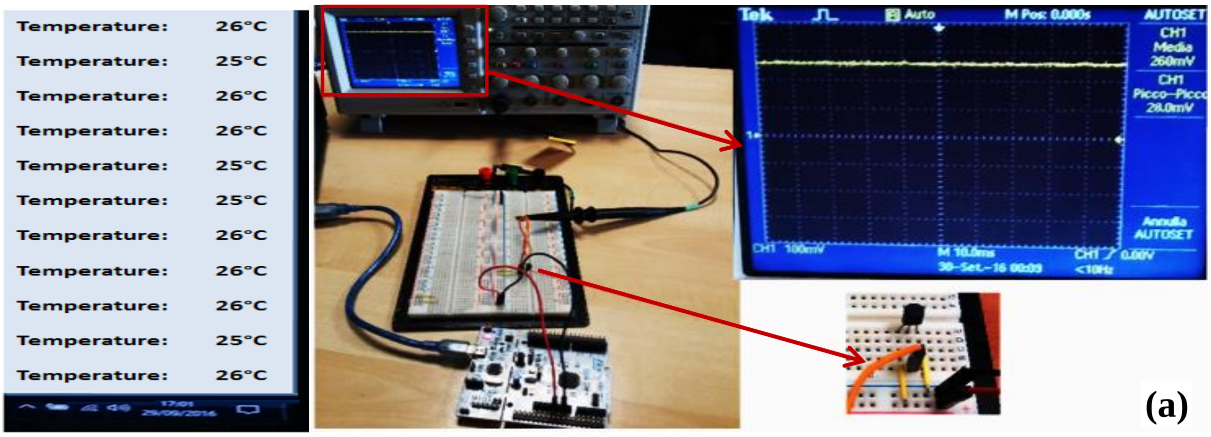

```
Temperature:    26°C
Temperature:    25°C
Temperature:    26°C
Temperature:    26°C
Temperature:    25°C
Temperature:    25°C
Temperature:    26°C
Temperature:    26°C
Temperature:    26°C
Temperature:    25°C
Temperature:    26°C
```

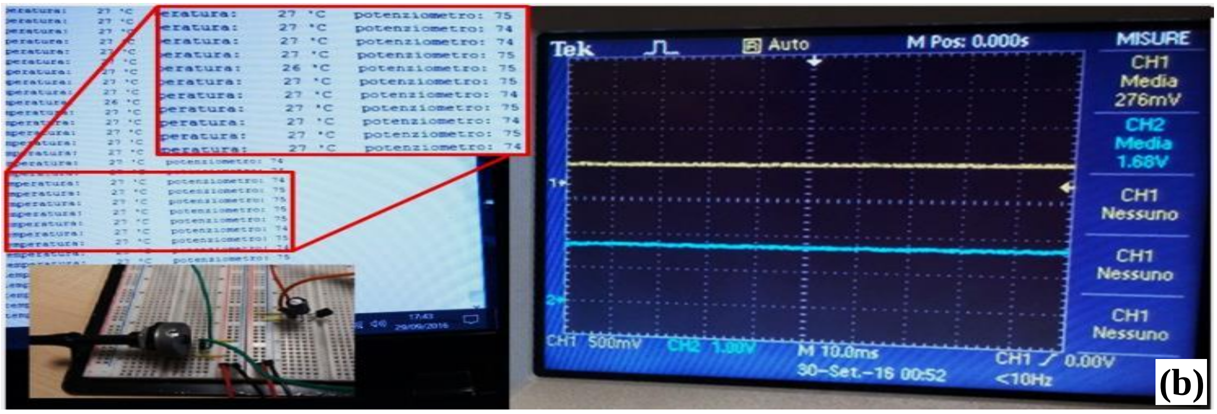

```
eratura:     27 °C   potenziometro: 75
eratura:     27 °C   potenziometro: 74
eratura:     27 °C   potenziometro: 74
eratura:     27 °C   potenziometro: 75
eratura:     26 °C   potenziometro: 75
eratura:     27 °C   potenziometro: 75
eratura:     27 °C   potenziometro: 74
eratura:     27 °C   potenziometro: 75
eratura:     27 °C   potenziometro: 74
eratura:     27 °C   potenziometro: 75
eratura:     27 °C   potenziometro: 74
```

Figure 27. Experimetal setup for verifying the correct operation of LM35 temperature sensor; analog signal is acquired/processed by ST Nucleo board and displayed on PC (on the left); the oscilloscope shows the voltage value provided by sensor (at 263mV corresponds $T_{amb}$ = 26°C).

The following test was related to the verification of reading operation, performed by ADC of ST Nucleo board, from two different sensors, one LM35 sensor and the other a potentiometer, connected to two different analog input pins of the board itself. Potentiometer was connected between 3.3V and ground, the third mobile connector applied to the PA1 input pin of the ST Nucleo board, whereas the LM35 sensor to the PC4 analog pin. During the test, it was observed that the temperature values reported on PC depended on the voltage value provided by potentiometer, even if the voltage values acquired by the oscilloscope were correct for both the analog inputs. This issue was overcome by connecting a capacitor, between the output pin of each LM35 temperature sensor and ground, so solving the observed problem of signals coupling between the analog input channels and also reducing possible noise contributions.

A further performed test was related to the proper functioning verification of the CHERRY GS1001 Hall sensors; a professional angular speed sensor was adopted to compare provided rpm values related to the revolutions counting for each minute, performed by a phonic wheel, with those provided by the Hall sensor. This last was connected to the ST Nucleo board and positioned to correctly detect the wheel rotation; the phonic wheel was mounted to a drill for easy activation of the revolutions to be counted. Thus, the proper functioning of the CHERRY GS1001 Hall sensor and the communication with the STM Nucleo board were checked, by comparing the acquired values with those detected by the professional sensor (see Figure 28). As reported in the Figures 28b and c, detected speed values of the phonic wheel by the Hall sensor correspond to the value visualized on display of the professional sensor (i.e. 194 rpm). In this experimental test, the Hall sensor was directly connected to the ST Nucleo board for verifying its proper functioning but, in the realized telemetry system, Hall sensors are connected to the engine control unit and then, through the Sparkfun CAN module, to the Nucleo board.

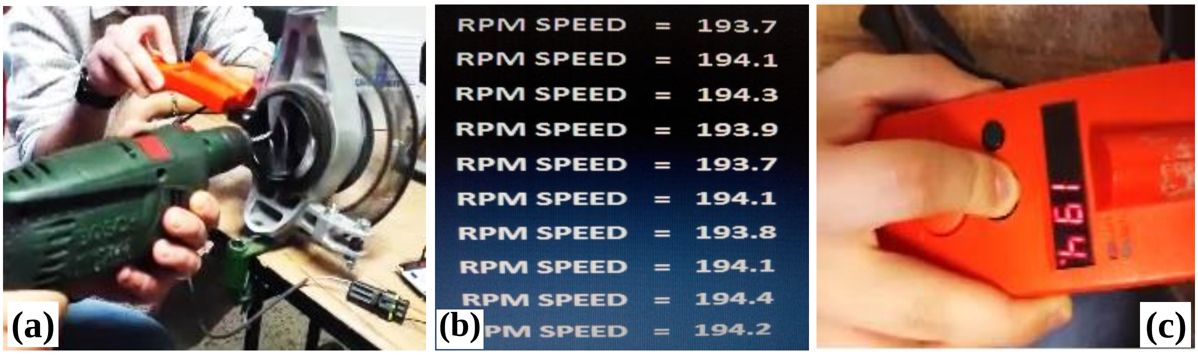

```
RPM SPEED  =  193.7
RPM SPEED  =  194.1
RPM SPEED  =  194.3
RPM SPEED  =  193.9
RPM SPEED  =  193.7
RPM SPEED  =  194.1
RPM SPEED  =  193.8
RPM SPEED  =  194.1
RPM SPEED  =  194.4
RPM SPEED  =  194.2
```

Figure 28. Photos related to experimental tests for operation verification of the Hall effect sensors (a); the speed values acquired by the Hall sensors and displayed on PC (b) are in agreement with the rpm value measured, at the same time, by using a professional sensor (c).

Later, the functional test of the Sparkfun CAN module was carried out; for this purpose, the cooling liquid temperature was acquired during the engine operation, by means of the HONDA NTC thermistor directly connected to the engine control unit; then detected data, through the Sparkfun CAN module, were provided to the ST Nucleo board, to be analyzed and displayed by the PC. These data were also stored on the SD memory card for verifying the proper operation of the Sparkfun CAN module; both functions, related to data acquisition from NTC thermistor and data storage were successfully performed [36-38].

Last functional test concerned the DORJI DRF1278F WiFi radio module operation; a simplex communication protocol was used (one module in transmission and the other in reception phase). The data packets were transmitted every 10ms; it was chosen a place with presence of some buildings, to test the WiFi transmission in the worst case, taking into account that, in the racing tracks, usually there are not buildings or interferences. By the perfomed wireless communication tests, the maximum distance between the transmitting and receiving WiFi modules to avoid data losses, was 1.2 km (see Figure 29); this result is satisfactory considering the presence of some buildings and that the distance target to reach was ≈ 600-800m.

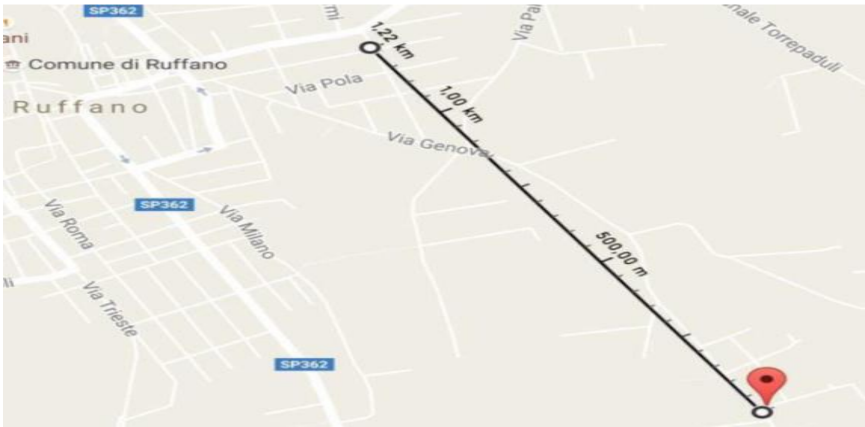

Figure 29. Map of town place where wireless communication tests were performed; maximum distance between the WiFi modules, to avoid data losses was 1.2 km, as indicated by pointer.

## VII. FUNCTIONAL TESTING OF THE COMPLETE TELEMETRY SYSTEM INSTALLED ON THE FSAE PROTOTYPE DURING ITS MOTION

The realized vehicle monitoring and wireless data transmission system, installed on the FSAE prototype car for its telemetry, is shown in Figure 30. Its main sections are indicated in the red rectangles; the ST Nucleo board and Sparkfun CAN bus modules are clearly visible on top of the board and also the ST HCF4051 multiplexer for selecting the desired LM35 sensor is highlighted. Furthermore, two black connectors, on the left side, are used for the connections with all sensors installed on the vehicle. Different pins of the two connectors were left free, to have the possibility to easily make modifications and improvements or to add further sensors.

On the realized PCB for conditioning of the sensors signals, also different components, i.e. capacitors and resistors, are mounted for adjusting the signals level for STM Nucleo board.

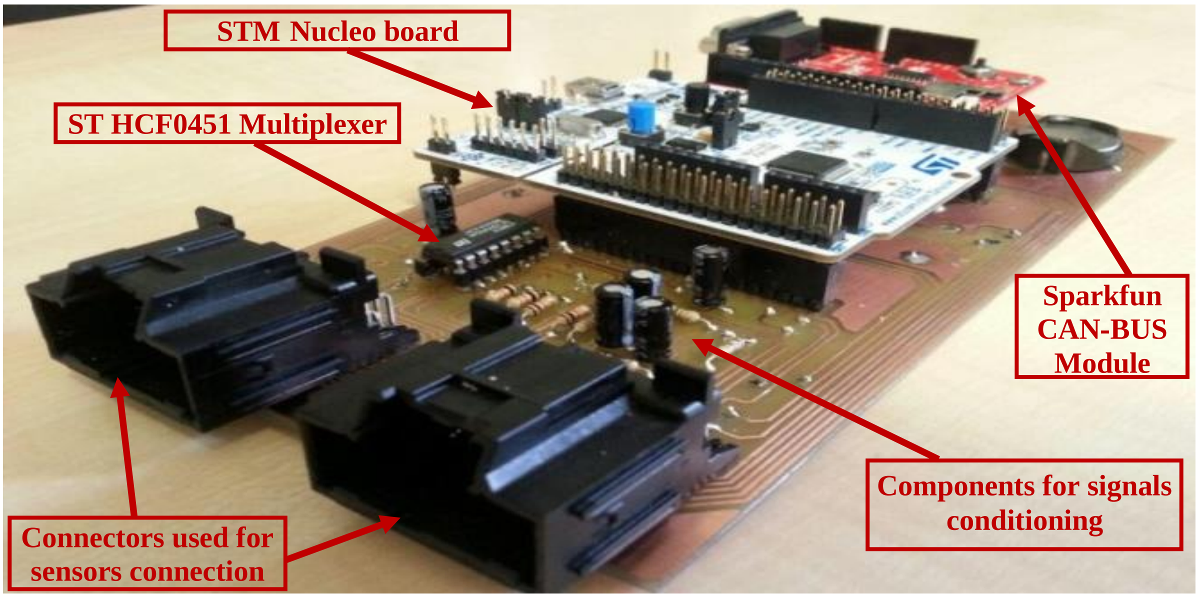
STM Nucleo board
ST HCF0451 Multiplexer
Sparkfun CAN-BUS Module
Components for signals conditioning
Connectors used for sensors connection

Figure 30. Lateral view of the realized sensors data acquisition and transceiver board: the ST Nucleo and CAN modules assembled on top, WiFi module not connected for a better visibility.

Transmitted data are received wirelessly from the base station, by using another DORJI DRF1278F WiFi radio module connected to a STM Nucleo board, where are visualized on PC terminal to be analyzed by the technical staff. The Figure 31 reports the graph of vehicle speed during the carried out test for 10 minutes. The speed values are acquired from the CHERRY GS1001 Hall sensors, each mounted in front of a phonic wheel attached on both the rear and front car wheels, as described previously. These data are then processed by the engine control unit for conversion operation (from the teeth number passing in front of Hall sensor per second, to vehicle speed value in km/h) and then received, through the Spurkfun CAN BUS module, from the ST Nucleo board. After, data are sent wirelessly to the base station via the

DORJI WiFi module. In Figure 31, the calculated speed of front (*hallf*) and rear (*hallr*) wheels, from the same side of the vehicle, are plotted for a time interval of 600 seconds; the vehicle speed is slowly increased, reaching 20 km/h, for the first 3 minutes, then, it is increased faster up to 60 km/h after about 3.5 minutes (220 seconds). Subsequently, a decelaration phase determines a speed decrease up to ≈ 20 km/h and an acceleration phase, between 280 and 330 seconds, causes a speed increase up to 65 km/h; then, after a deceleration, the vehicle is stopped, as highlighted in the graph at about 7 minutes (410 seconds). The test continues with an acceleration and deceleration phase before stopping the vehicle again.

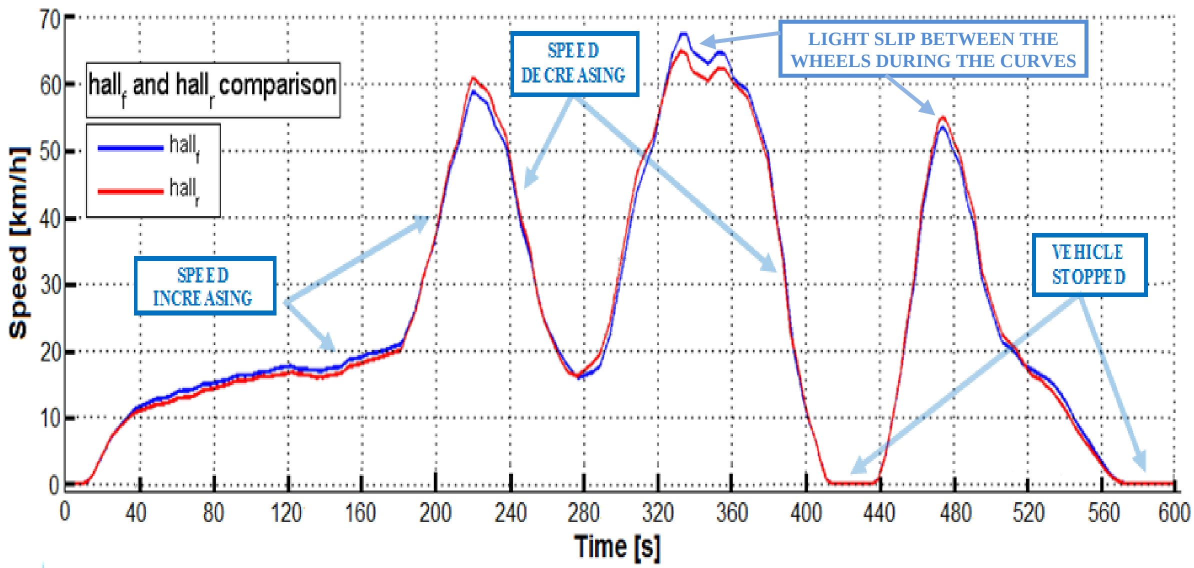

Figure 31. Graph related to speed data received wirelessly from base station (for 10 min); the curves show acceleration and deceleration phases or vehicle stopping (speed values ≈ zero). Blue curve related to Hall sensor mounted on front wheel, red curve for sensor on rear wheel.

Received data show that the two Hall sensors, mounted on the two wheels, are functioning properly; in fact, the two curves are overlapped, reporting rpm speed for both rear and front wheels. In some intervals, for example between 320 and 360 seconds, a slight slip is present due to uneven asphalt conditions, to pilot maneuvers or if vehicle is going through a curve.

Received data confirm also the proper functioning of the IXTHUS linear potentiometers, thus allowing to establish the behavour of vehicle suspensions and therefore to monitor their integrity and road conditions. The linear potentiometers are directly connected to the STM Nucleo board; it acquires the analog signals provided by potentometers and, after a processing phase to obtain the extension value expressed in mm, by using the WiFi radio module, it sends the extension data to the base station. Figure 32 reports the obtained curve related to the extension (mm) of the front left and front right suspensions of the vehicle, for a time interval of 400 seconds. It is crearly visible the compressions and extensions of the two potentiometers, when vehicle is running a curve on the right or on the left. When the vehicle curves on the left, the extension of front-left potentiometer and compression of the other one occur, vice-versa when the curve is on the right (for example between 340 and 360 seconds); otherwise, the potentiometers position stabilizes around 18 mm. The potentiometers provide their analog output, related to the detected extension value, to the STM Nucleo board which converts, as previously illustrated, the acquired values in the extension values in mm. In the obtained graph, the maximum extension and compression of the two potentiometers (of about 6mm) is around 310 seconds, when the pilot performs an abrupt steering on the left with the resulting behaviour, monitored by means of the telemetry system, of the vehicle suspensions.

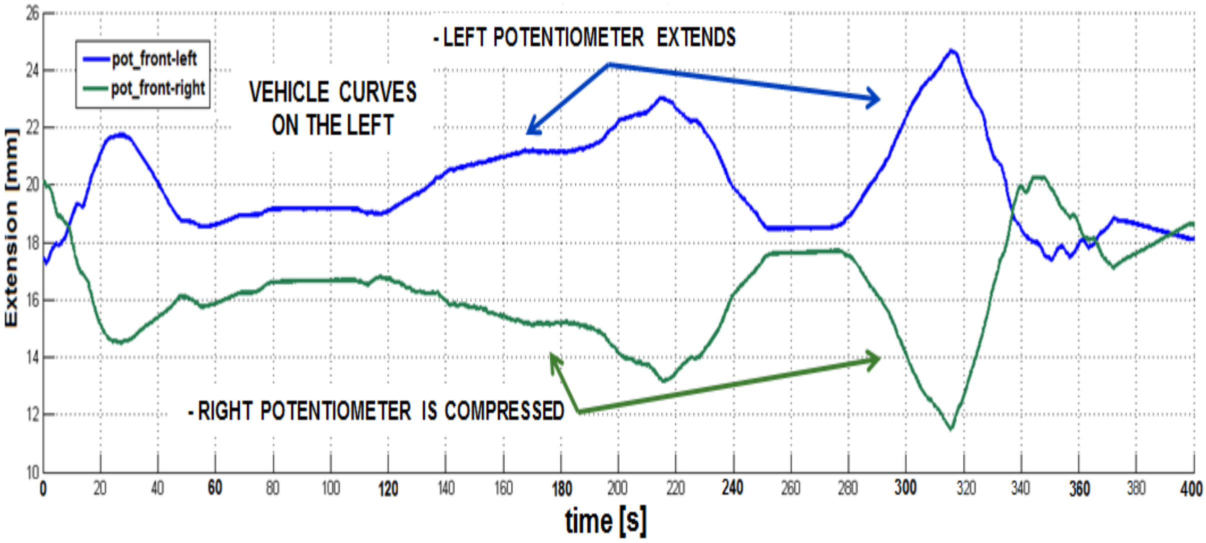

Figure 32. Graph related to suspensions extension in the time interval [0 - 400] sec; obtained curves of the left and right potentiometers present, as expected, a symmetric behaviour.

Figure 33 reports the plot of detected data related to the cooling liquid temperature; the curve shows the liquid temperature variation as function of the RPM engine. First to start moving, the vehicle remains stopped (engine off) for the first 600 seconds and the detected temperature value is of 23°C; subsequently, when the vehicle starts movement, the acceleration causes the liquid temperature increase, that reaches, after about 300 seconds, ≈ 72°C.

The liquid temperature value remains around 71°C in the time interval between 900 - 1200 seconds and around 82°C between 1350 - 1650 seconds, while the engine RPM values are maintained constant. When engine RPM are increased, the liquid temperature reaches 90-95 °C; obtained data confirm that the Honda NTC thermistor, connected to the engine control unit, detects correctly the temperature value of cooling liquid that never goes beyond 90-95°C. Thus, data are properly acquired by the data acquisition and wireless communication system, installed on the vehicle, and correctly sent to base station to be plotted as shown in Figure 33.

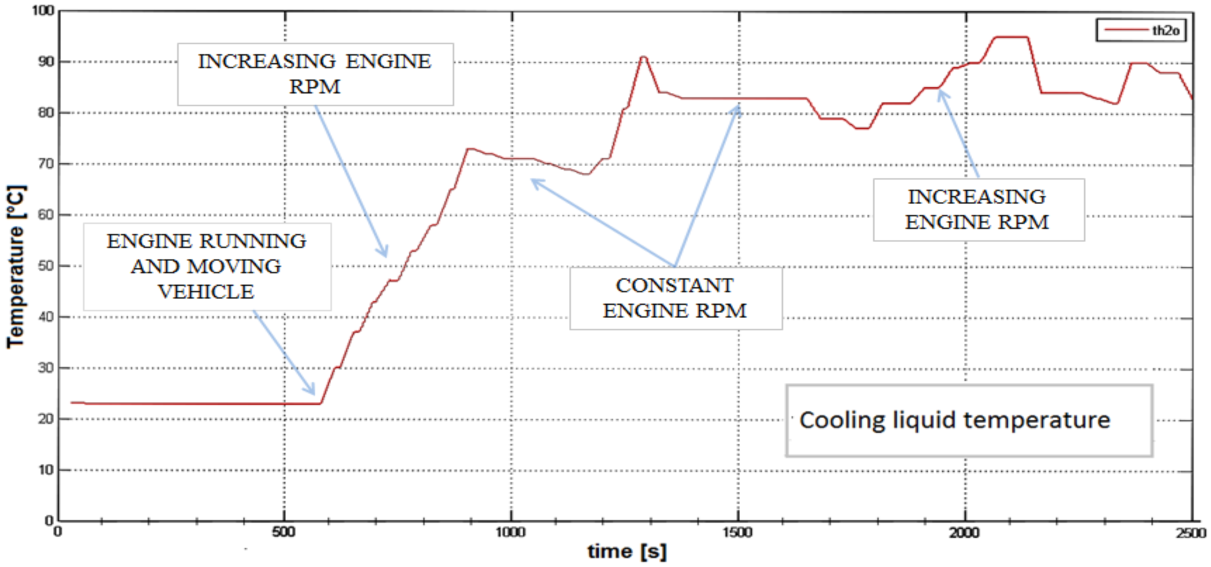

Figure 33. Time-domain plot of the cooling liquid temperature; the detected values increase starting from 600sec, when vehicle starts movement, in accordance to engine rpm variation.

The next Figure 34 regards data provided by the four LM35 temperature sensors located into the engine compartment; they are directly connected to the ST Nucleo board, which acquires and processes the analog values provided as output after selecting, through the ST HCF4051 multiplexer, each LM35 sensor. The test was carried out with moving vehicle for about 9 minutes, whereupon the vehicle was stopped. As reported in the graph, in correspondence of a deceleration phase but with high rpm engine values (range [500 – 550]sec), the temperature of engine compartment increases; in fact, the wind investing moving vehicle allows to keep low the engine compartment temperature, but being reduced then a temperature rising occurs.

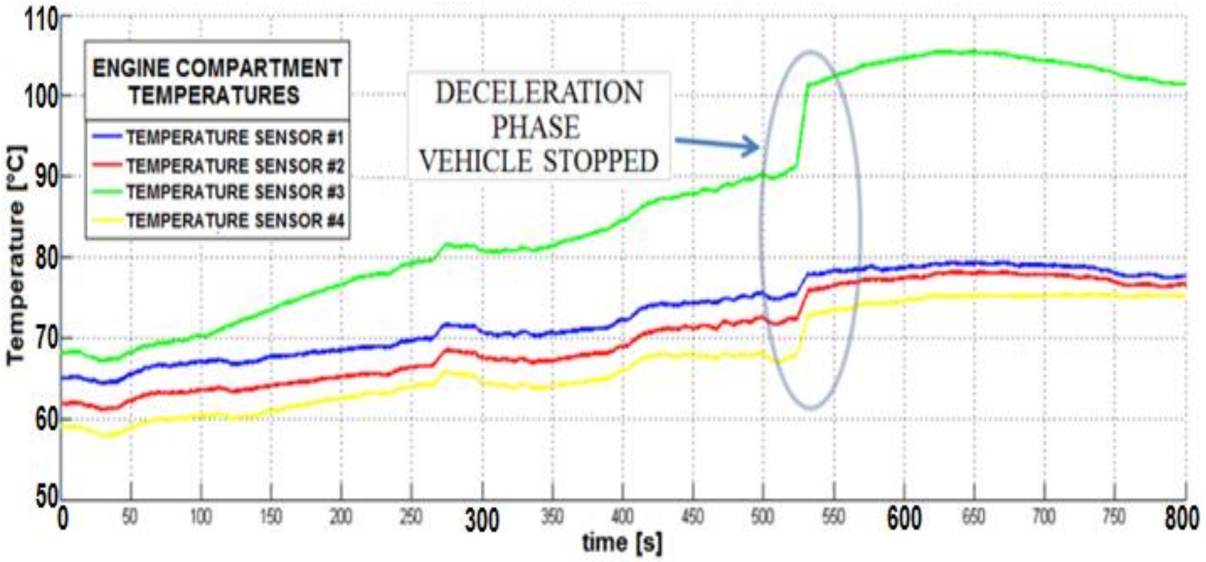

Fig. 34. Curves of the engine compartment temperatures; the detected values increase in correspondence of deceleration phases and with vehicle stopped (but with high rpm engine values, in these phases) due to the wind reduction.

All LM35 sensors detect a temperature value of about 75-80°C except for one sensor, corresponding to the green curve, which is located close to the exhaust pipe and detects a temparature value higher up to 105°C.

Finally, Figure 35 reports the acceleration values detected from the MPU6050 gyroscope/ accelerometer sensor installed at the center of the vehicle. The plotted curve shows a slight acceleration at the beginning, when the vehicle starts the movement and then an acceleration after 180 seconds, as expected by comparing the acceleration trend with that related to vehicle speed, shown in Figure 31, where the speed value, between 180 and 220 seconds, increases up to 60 km/h. Subsequently, several acceleration and deceleration phases are performed by the pilot as function of the road conditions and the track shape, i.e. curves or straights.

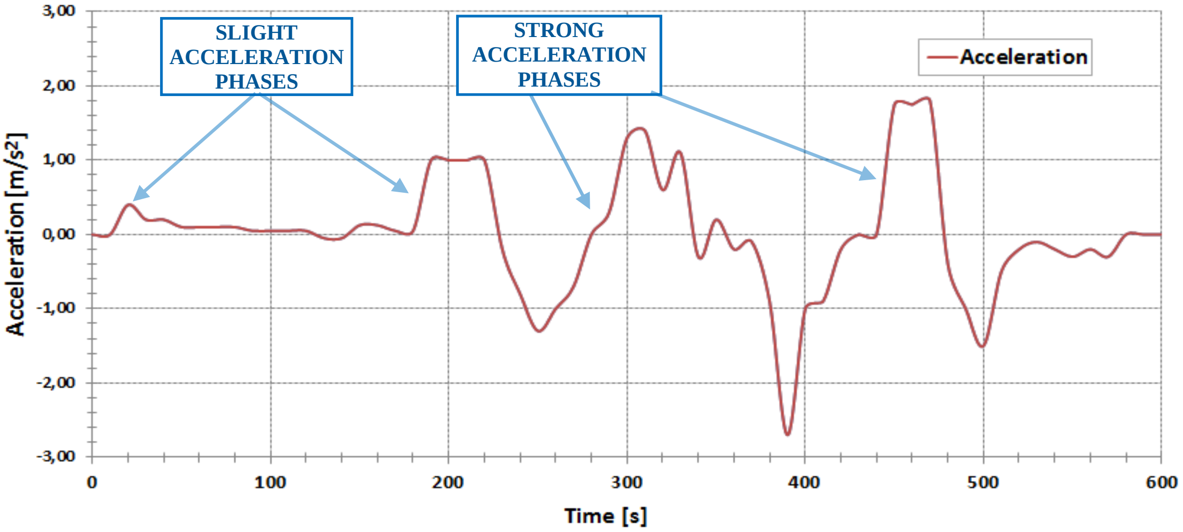

Figure 35. Curve related to vehicle acceleration obtained from data acquired by the MPU6050 gyroscope/accelerometer sensor and sent wirelessly to the base station, to be analyzed.

Figure 37 reports the angular velocity of yaw as deteced by the MPU6050 sensor; before to analyze the related curve, we consider the following Figure 36 with drawn the pitch, roll and yaw axes, related to the vehicle dynamics. The roll-motion axis extends through the center of the vehicle (X axis in green), pitch-motion axis through the sides of vehicle (Y axis in red), and finally, the yaw is the moment about the axis protruding through the roof of vehicle (the Z vertical axis in blue colour). Thus, yaw angle detects the curves of road crossed from vehicle.

As reported in the paragraph IV, the MPU6050 sensor consists of three independent vibratory MEMS rate gyroscopes, which detect rotation about the X, Y, and Z axes. When the gyros are rotated about any of the sense axes, the Coriolis Effect causes a vibration that is detected by a capacitive pickoff transducer, as explained in the datasheet [25]. The MPU6050 sensor, after a processing phase of acquired rotational data, provides the angular velocity expressed in deg/sec.

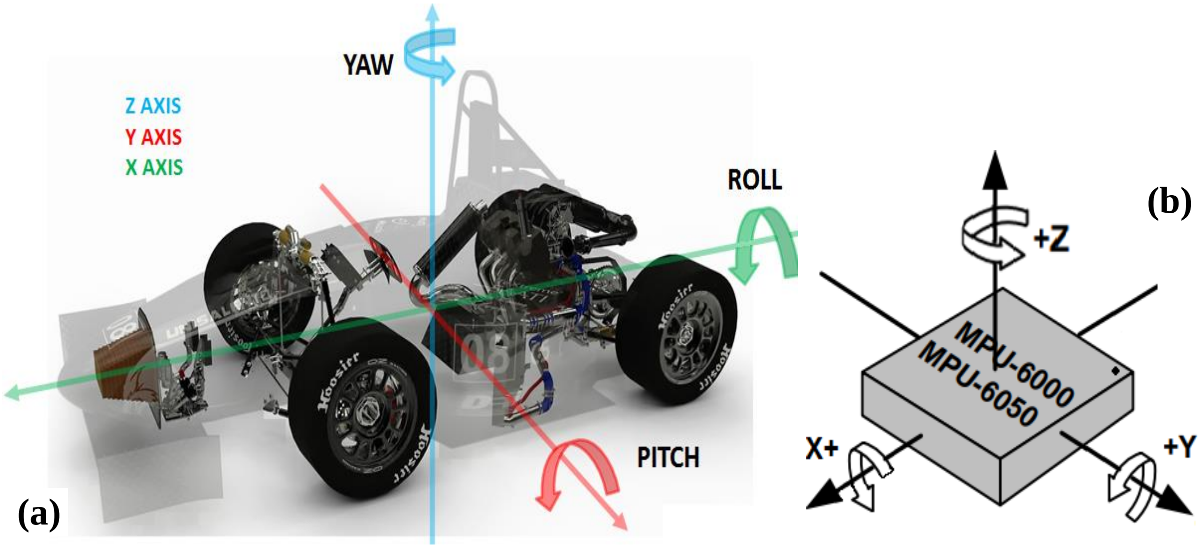

Figure 36. Graphic representation of the three axis, roll, pitch and yaw, related to vehicle dynamics (a) and related orientation of MPU6050 sensor located at the center of vehicle (b).

The Figure 37 reports the values, as acquired and processed from the MPU6050 gyroscope/ accelerometer sensor, of the angular velocity related to the yaw axis. A yaw rotation is a movement around the yaw axis of a rigid body that changes the direction it is pointing, to the left or right of its direction of motion (as shown in Figure 36). The yaw rate or yaw velocity of a vehicle, aircraft, projectile or other rigid body is the angular velocity of this rotation. Therefore, by comparing the obtained curve with that related to vehicle speed (Figure 31), it is clearly visible, for example around 280 seconds, the speed decreasing and contemporary yaw angle variation, indication of the presence of a curve; this is also highighted in other points of the yaw and speed curves (e.g between 180 and 190 seconds or from 480 to 500 seconds).

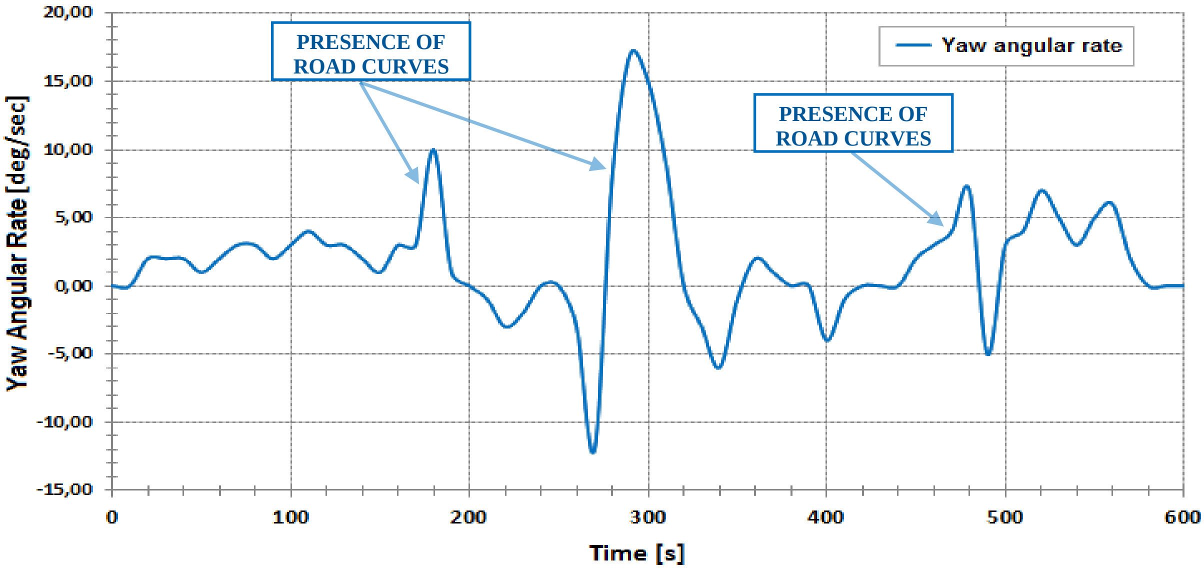

Figure 37. Graph of the yaw angular velocity, as detected from the MPU5060 sensor during the vehicle motion, with highlighted the time intervals when the vehicle is running a curve.

The carried out experimental tests have demonstrated that the realized telemetry system is able to reliably monitor in real time the different parameters of the FSAE vehicle during its motion, by using sensors and commercial electronic boards available on the market at very low cost. The detected sensors data related to vehicle speed, to linear potentiometers mounted on the wheels suspensions, to cooling liquid and engine compartment temperatures, to vehicle acceleration and inclination angles are correctly received wirelessly from the receiving unit located into the base station, where can be analyzed by the technicians, in order to ensure the pilot safety, quick interventions in case of malfunctions and obviously high FSAE vehicle performances.

## VIII. CONCLUSIONS

The *Salento racing team*, a group of researchers and students of Salento University, realized the SRT16 prototype single-seater car to partecipate to the Formula SAE races. In this paper, the related telemetry system was presented, able to monitor in real time and continuously the physical and mechanical parameters of the vehicle moving, by a remote base station. The telemetry system plays a key role to safeguard the pilot life and to optimize vehicle performances; it is composed of different sensors installed on vehicle, namely temperature sensors for the engine operation control, thermistor for cooling liquid temperature, Hall-effect speed sensors positioned on car wheels, linear potentiomenters for measuring the suspensions extension and finally a 3-axis gyroscope/accelerometer sensor for detecting acceleration and inclination angles (i.e. pitch, roll and yawing). All data coming from mentioned sensors are acquired by ST Nucleo board which, by using a DRF1278F WiFi module properly connected to the ST board, sends them to another WiFi module located into the base station; here, the received sensors data are visualized on PC terminal, by means of a second ST Nucleo board connected via USB to PC, for technicians analysis. The developed firmware, installed into microcontroller on board of ST Nucleo board, allows to acquire the digital data and analog signals from used sensors by synchronizing all operations, to perform the needed convertion operations and to interface the ST board itself with all other electronic modules. Performed experimental tests demontrated that the telemetry system works properly; all received data from base station are in accordance between themselves, reporting correctly and in real-time the monitored vehicle parameters as function of different track conditions and vehicle status.

## REFERENCES

[1] E. Önler, S. Çelen, A. Moralar, İ. H. Çelen: Development of Telemetry System for Electric Powered Vehicle. Int. Journal of Current Research, Vol. 8 (9), pp. 38715-38719 (2016).

[2] P. Taylor, N. Griths, A. Bhalerao, S. Anand, T. Popham, Z. Xu, A.Gelencser: Data Mining for Vehicle Telemetry. Applied Artificial Intelligence, Vol. 30 (3). pp. 233-256, 2016.

[3] Y. Zhu, N. Kang, J. Cao, A. Greenberg, G. Lu, R. Mahajan, D. Maltz, L. Yuan, M. Zhang, B. Y. Zhao, H. Zheng: Packet-Level Telemetry in Large Datacenter Networks. Proc. of the 2015 ACM Conf. on Special Interest Group on Data Communication, (SIGCOMM '15), pp. 479-491, London (UK), DOI: 10.1145/2785956.2787483, 2015.

[4] J. Elliott: Telemetry helps Formula SAE team close the loop on design. SAE International, http://articles.sae.org/11264/, 07 Aug 2012.

[5] P. Primiceri, P. Visconti, A. Melpignano, A. Vilei. G. M. Colleoni: Hardware and software solution developed in ARM mbed environment for driving and controlling DC brushless motors based on ST X-NUCLEO development boards. International Journal on Smart Sensing and Intelligent Systems, Vol. 9 (3), pp.1534–1562, Sept. 2016.

[6] P. Visconti, R.de Fazio, P. Primiceri, A. Lay-Ekuakille: A solar-powered White LED based UV-VIS spectrophotometric system managed by PC for air pollution detection in faraway and unfriendly locations. International Journal on Smart Sensing and Intelligent Systems, Vol. 10 (1), pp. 18 - 48, (2017).

[7] P. Visconti, R. Ria, G. Cavalera: Development of smart PIC-based electronic equipment for managing and monitoring energy production of photovoltaic plan with wireless transmission unit. ARPN Journal of Engineering and Applied Sciences. Vol. 10 (20), pp. 9434 – 9441 (2015).

[8] P.Visconti, P. Primiceri, P.Costantini, G.Colangelo, G. Cavalera: Measurement and control system for thermo-solar plant and performance comparison between traditional and nanofluid solar thermal collectors"; Int. Journal on Smart Sensing and Intelligent Systems, Vol. 9 (Issue 3), pp. 1220 – 1242, http://s2is.org/Issues/v9/n3/papers/paper3.pdf (2016).

[9] P. Visconti, G. Giannotta, R. Brama, P. Primiceri, A. Malvasi: Features, operation principle and limits of SPI and I2C communication protocols for smart objects: a novel SPI-based hybrid protocol especially suitable for IoT applications. International Journal on Smart Sensing and Intelligent Systems, Vol. 10 (2), pp. 262 - 295, (2017).

[10] P. Visconti, P. Primiceri, G. Cavalera: Wireless monitoring system of household electrical consumption with DALY-based control unit of lighting facilities remotely controlled by Internet. J. of Communications Software and Systems, Vol. 12 (1), pp. 4 - 15, (2016).

[11] P. Visconti, P. Primiceri, C. Orlando: Solar Powered Wireless Monitoring System of Environmental Conditions for Early Flood Prediction or Optimized Irrigation in Agriculture. ARPN Journal of Engineering and Applied Sciences, Vol. 11 (Issue 7), pp. 4623-4632, (2016)

[12] P. Visconti, A. Lay-Ekuakille, P. Primiceri, G. Cavalera: Wireless Energy Monitoring System of Photovoltaic Plants with Smart Anti-Theft solution integrated with Household Electrical Consumption's Control Unit Remotely Controlled by Internet. International Journal on Smart Sensing and Intelligent Systems, Vol. 9 (Issue 2), pp. 681 – 708 (June 2016).

[13] CAEMAX imc group, Dx: Digital Multi-Channel Telemetry System, Technical Data Sheet 1.6, Feb. 2017 -Available Online: http://www.caemax.de/en/products/telemetry/dx/.

[14] KTM Kraus Messtechnik GmbH, Telemetry for Automotive Testing - [Online]. Available: http://www.kmt-telemetry.com/applications-measurement/automotive/

[15] KTM - Kraus Messtechnik GmbH, Telemetry, CT4/8 –Wheel / Rotate - 4 (8) Channel Wheel Telemetry System, Datasheet Version 2015, 12. Available online: http://www.kmt-telemetry.com/fileadmin/media/Downloads/Rotating/CT4-8-Wheel-DS.pdf .

[16] Magneti Marelli S.p.A, Motorsport. Available online: http://www.magnetimarelli.com/business_areas/motorsport .

[17] Accumetrics, Inc., AT-5000 EasyApp, Battery Powered Rotor Telemetry System 2017, Datasheet Available online: http://www.accumetrix.com/contentStore/mktg/Accumetrix/PDF/Accumetrics_AT5000_Datasheet.pdf.

[18] ST Microelectronics, STM32 Nucleo-64, Datasheet ID 025838, Rev 8, pp. 1-5, 2016. http://www.st.com/content/ccc/resource/technical/document/data_brief/c8/3c/30/f7/d6/08/4a/26/DM00105918.pdf/files/DM00105918.pdf/jcr:content/translations/en.DM00105918.pdf.

[19] M.Santhosh Kumar, C.R. Balamurugan: Self - Propelled Safety System Using CAN Protocol-A Review. World Conference on Futuristic Trends in Research and Innovation for Social Welfare. Coimbatore (India), DOI: 10.1109/STARTUP.2016.7583899 (2016).

[20] P. Nawale, A. Vekhande, P. Waje: Vehicle Parameter Monitoring Using CAN Protocol. International Journal of Computer Science Trends and Technology (IJCST), Vol. 3 (1), pp. 46-49 (2015).

[21] R. M. Prasanth, S. Raja, L. Saranya: Vehicle Control Using CAN Protocol For Implementing the Intelligent Braking System (IBS). Int. Journal of Advanced Research in Electrical, Electronics and Instrumentation Engineering, Vol.3 (3), pp. 7597-7605 (2014).

[22] SparkFun Electronics, CANBUS Shield DEV13262. Available online: https://www.sparkfun.com/products/13262.

[23] Gefran spa, PZ12 Rectilinear Displacement Transducer with Cylindrical Case, - [Online]. Available: https://gefran-online.com/pz12-rectilinear-displacement-transducer-with-cylindrical-case.html.

[24] Switches and Sensors (ZF) – Fromerly Cherry Switches, GS1001 – GS1002 SENSORS, Datasheet online: http://switches-sensors.zf.com/us/wp-content/uploads/sites/7/2012/05/GS1001- GS1002_Geartooth_Speed_Sensor_Datasheet_Letter.pdf.

[25] TDK InvenSense Inc., MPU-6000 and MPU-6050 Product Specification Revision 3.4, Document Number: PS-MPU-6000A-00, 08/19/2013. Available online: https://www.invensense.com/wp-content/uploads/2015/02/MPU-6000-Datasheet1.pdf.

[26] DORJI Applied Technologies, DRF1278F 20dBm LoRa Long Range RF Front-end Module V1.11, Revision 1.1, pp. 1-6, Aug. 2015. Available online: http://www.dorji.com/docs/data/DRF1278F.pdf.

[27] SEMTECH, Wireless, Sensing & Timing LoRa, SX1276/77/78/79 - 137 MHz to 1020 MHz Low Power Long Range Transceiver, Datasheet, Revision. 5 Aug. 2016. Available online: http://www.semtech.com/images/datasheet/sx1276_77_78_79.pdf.

[28] SEMTECH, Wireless, Sensing & Timing Products, AN1200.22 LoRa™ Modulation Basics, Appl. Note, Rev. 2 May 2015. Available online: http://www.semtech.com/images/datasheet/an1200.22.pdf.

[29] A. Augustin, J. Yi, T. Clausen, W.M. Townsley: A Study of LoRa: Long Range & Low Power Networks for the Internet of Things. Sensors, Vol. 16, pp 1466 (1-18), (2016).

[30] P.Visconti, P. Primiceri, G. Cavalera: Wireless Monitoring and Driving System of Household Facilities for Power Consumption Savings Remotely Controlled by Internet. IEEE Proc. of 2016 IEEE Workshop on Environmental, Energy and Structural Monitoring Systems, (EESMS), Bari (Italy), 13-14 June 2016, DOI: 10.1109/EESMS.2016.7504805, (2016).

[31] P. Primiceri, P. Visconti: Solar-powered LED-based Lighting Facilities: an Overview on Recent Technologies and Embedded IoT Devices to obtain Wireless Control, Energy

Savings and Quick Maintenance. ARPN Journal of Engineering and Applied Sciences, Vol. 12 (1), pp. 140-150, (2017).

[32] P. Visconti, A. Lay-Ekuakille, P. Primiceri, G. Ciccarese, R. De Fazio: Hardware Design and Software Development for a White LED-Based Experimental Spectrophotometer Managed by a Pic-Based Control System. IEEE Sensors Journal, Vol. 17 (8), pp. 2507 – 2515, (2017).

[33] D. Nakhaeinia, P. Payeur, A. Chávez-Aragón, A. M. Cretu, R. Laganière, R. Macknojia: Surface Following with an RGB-D Vision-Guided Robotic System for Automated and Rapid Vehicle Inspection. International Journal on Smart Sensing and Intelligent Systems, Vol. 9 (2), pp. 419 – 447, (2016).

[34] Y. Qiang, L. Chen, L. Hua, J. Gu, L. Ding, Y. Liu: Research on the Classification for Faults of Rolling Bearing Based on Multi-Weights Neural Network. International Journal on Smart Sensing and Intelligent Systems, Vol. 7 (3), pp. 1004 – 1023, (2014).

[35] S. K. Gharghan, R. Nordin, M. Ismail: Development and Validation of a Track Bicycle Instrument for Torque Measurement Using the Zigbee Wireless Sensor Network. International Journal on Smart Sensing and Intelligent Systems, Vol. 10 (1), pp. 124 – 145, (2017).

[36] S. H. Teay, C. Batunlu, A. Albarbar: Smart Sensing System for Enhancing the Reliability of Power Electronic Devices used in Wind Turbines. International Journal on Smart Sensing and Intelligent Systems, Vol. 10 (2), pp. 407–423, (2017).

[37] J. Renxia, Y. Hongguan, W. Li, C. Lihui: Errors of Manometric $CO_2$ Sorption Experiments on Coal Caused by Accuracy of Pressure Sensor. International Journal on Smart Sensing and Intelligent Systems, Vol. 9 (2), pp. 468–490, (2016).

[38] C. Doyle, D. Riordan, J. Walsh: A Cost-Effective and Accurate Electrical Impedance Measurement Circuit Design for Sensors. International Journal on Smart Sensing and Intelligent Systems, Vol. 9 (2), pp. 509–525, (2016).